BTK-NLRP3-Caspase1 and Gasdermin D-Caspase 11 pathways jointly drive neuroinflammation and functional impairments in a rat model of psychosocial stress

Soni Tiwari[1,2, 3*], Zaidan Mohammad[1,4*], Santi Ranjan Atta[1,2], Shweta Kaushik[2] Aryan Tiwari[1], Amla Chopra[3], Itender Singh[2,5], Simantini Ghosh [1]

1- Department of Psychology, Ashoka University, Rai, India
2- Ambedkar Centre for Biomedical Research, Delhi University, New Delhi, India
3- Department of Zoology, Dayalbagh Education Institute, Dayalbagh, Agra, India
4- University of Vermont , Burlington VT, USA
5- Department of Neurosurgery, Washington University School of Medicine in St. Louis, St. Louis, MO, USA.

*Equal contribution

Correspondence to Simantini Ghosh (simi@ashoka.edu.in)

ORCID

Soni Tiwari: 0009-0008-7289-541X

Zaidan Mohammad: 0000-0002-1404-2653

Santi Ranjan Atta: 0009-0004-5592-1437

Shweta Kaushik: 0009-0007-6780-9268

Aryan Tiwari: 0009-0006-6118-3471

Amla Chopra: 0000-0002-6859-6643

Itender Singh: 0000-0002-5117-0814

Simantini Ghosh : 0000-0002-0791-7255

Abstract

Common psychological disorders related to stress, depression and anxiety pose serious disease and economic burden globally and especially in lower and lower middle-income countries. Existing pharmacotherapies mostly target neurotransmitter systems and are partially effective across a range of diagnostic categories. However, it is also a long-standing finding that a low grade inflammation in persistently present in systemic circulation as well as in the brain in stress, depression and anxiety. Specifically, neuroinflammation driven by Interleukin-1β (IL-1β) a pleiotropic cytokine. has recently been the focus of keen interest in stress, depression and anxiety research. IL-1β is probably the most prominent proinflammatory cytokine in the brain and has been long associated with these conditions. We focus on molecules that cause IL-1β to be synthesized from its precursor, namely Caspase 1, through activation of a large multiprotein complex known as the NLRP3 inflammasome complex. Using two different rat models of physical and psychosocial stress, we validate our earlier findings of the induction of the BTK/NLRP3/Caspase 1 Canonical Pathway in stressed animals. We also show the involvement of Gasdermin D/ Caspase11 driven non canonical pathway that contributes to enhanced leakage of IL-1β from cells through pyroptosis, in the absence of lytic cell death. Stressed rats display a robust neuroinflammatory phenotype, reduction in CA3 Hippocampal spine density, as well as number of mature mushroom spines, and functional impairments across multiple domains of behavior. Finally we employ two FDA approved drugs, Ibrutinib and Disulfiram to partially mitigate the neural, neuroinflammatory phenotype as well as behavioral dysfunctions, individually and in combination. The combination therapy proved to be more efficacious, suggesting a joint inhibition of the canonical and non canonical pathway mitigates the pathological as well as behavioral sequelae of psychosocial stress. Taken together our data provides robust

preclinical data and argues for amelioration of the NLRP3 dependent IL-1β release to be considered as an alternative therapeutic strategy in stress, depression and anxiety.

Keywords*: Interleukin 1β, NLRP3, BTK, Gasdermin D, Social Defeat Stress, Ibrutinib, Disulfiram*

Introduction

The Global Burden of Disease (GBD) study conducted by the World Health Organization (WHO) assessing the burden of psychological disorders worldwide reported 15% of life years lost to these disorders (1), however, a more recent analysis has shown that this may have been underreported. When the definition is expanded, the epidemiological and economic burden of psychological disorders between 2000-2019 are even larger and is estimated at 418 million DALYS and about USD 5 trillion (2). Further GBD data that common psychiatric disorders related to anxiety, depression and traumatic stress constitute significantly to this burden and the burden of these disorders are disproportionately borne by lower and middle income countries (1,3,4), and anxiety related disorders in general have a much earlier onset compared to serious psychological disorders (5). The treatment gap is also extremely large in countries of the global south including India (6,7) yet research in common psychiatric disorders remain underfunded in comparison to other neuropsychiatric disorders (8) and the dominant form of pharmacological therapy for individuals with these disorders are limited to SSRIs and drugs that ultimately change different neurotransmitter levels in the brain, yet only have partial efficacy (9–15). The situation has been worsened globally by the pandemic, but predictably the lower middle income countries have once again borne the brunt of the exacerbation (16). Reporting of psychological disorders, compliance, cultural and economic barriers to seeking professional help, particularly in LMICS and LICS have been extensively studied by researchers across the globe. In face of this there is a need for a transdiagnostic approach towards pharmacotherapy across common

psychiatric disorders, that is also scalable and feasible. SSRIs are the usual choice for most anxiety and stress related disorders (17,18). Meta analyses indicate that SSRIs are linked with small to moderate effect sizes in anxiety disorders, PTSD and MDD (19–21) and are also linked with side effects despite their popularity (22–24). Given the scope and magnitude of the problem posed by common psychiatric disorders and the very large treatment gap, there is significant room to investigate therapeutic strategies that don't focus only on neuronal and neurotransmitter related correlates. Of particular interest here is the long-standing body of evidence that stress and anxiety related disorders as well as depression are marked by low grade inflammation, across human and animal studies across several diagnostic categories. Immune dysregulation marked by the enhanced presence of proinflammatory cytokines such as IL-1β. TNFα, and IL-6 is closely associated with PTSD, Depression and anxiety disorders (25–28). The production of these cytokines also strongly associate with symptom severity in both anxiety and depression (29).

Overarchingly our laboratory is interested in investigating therapeutic strategies that modulate these cytokines, specifically IL-1β, a major proinflammatory cytokine in the brain, and observing the results of this modulation, in models of stress and anxiety *in vivo*. IL-1β is known as a key mediator of neuroinflammation in neurodegeneration, traumatic brain injury and stroke with important role in pathophysiology (30–34). IL-1β increases the mRNA expression of multiple other genes across various cell types, including monocytes and macrophages and induces the expression of its own genes, creating a positive feedback loop (35–37).

It is in this context that we focus on the NOD-, LRR-, and pyrin domain-containing protein 3 (NLRP3) inflammasome, a multiprotein complex which is one among evolutionarily important and conserved PAMPS and DAMPS of the innate immune system and serves as

an upstream regulator of IL-1β production. NLRP3 inflammasome is characterised by an oligomeric structure, maintained in an inactive state via interactions among the C-terminal LRR domains. NLRP3 assembles with Asc and forms a supramolecular complex known as the inflammasome in reaction to specific stimuli, which activates caspase-1 and results in the secretion of interleukin (IL)-1β (38). The assembly of the NLRP3 inflammasome results in the caspase-1 dependent secretion of the pro-inflammatory cytokines IL-1β and IL-18, along with Gasdermin D (GSDMD)-mediated pyroptotic cell death (39). IL-1β is produced by the cysteine protease caspase-1 following the cleavage of its precursor protein Pro-IL1β, marking the final stage of the NLRP3 inflammasome activation (40). Aberrant activation of the NLRP3 inflammasome is linked to the pathogenesis of multiple inflammatory diseases, including diabetes, lifestyle conditions such as smoking cancer, and Alzheimer's disease (38). Recently, the NLRP3 inflammasome has been attracting attention in psychological disorder research as well (41–43). The NLRP3 inflammasome is elevated in the brain and blood of depressive patients (43,44) and is a key mediator of pro-inflammatory activity and the release of IL-1β in anxiety and depression (45–47). We have previously demonstrated that BTK acts as an upstream regulator of NLRP3 activation in mouse models of physical restrain stress, leading to upregulation in IL-1β as well as other neuroinflammatory mediators, with exacerbated anxious behavior, We also demonstrated that BTK inhibition with Ibrutinib led to amelioration of this heightened anxious phenotype with a concomitant reduction in neuroinflammation and IL1β mediated through NLRP3 activation(48). In this paper we extend our studies to further downstream effectors of this pathway and also investigate a second pathway that contributes to the final outcome of enhanced release of IL-1β.

NLRP3 inflammasome activation can happen through the canonical pathway that leads to enhanced formation of IL-1β from pro-IL-1β , cleaved by Caspase 1. However, Caspase 1

can also cleave another molecule Gasdermin D (GSDMD), a 480 amino acid long protein into an N-terminal fragment, that can lead to formation of small transmembrane pores that leads to leakage of more IL-1β into the interstitial space apart from its secretory release, disruption of ion and water regulation that eventually worsens inflammation and leads to cell death through a process named pyroptosis (49). GSDMD consists of two distinct domains interconnected by a linker region. Upon the assembly of inflammasomes, the linker region of GSDMD is cleaved by caspase-1 and leads to the formation of a noncovalent complex between the N terminus and the C terminus (50,51). The cleaved -N terminus can undergo auto-oligomerization on membranes upon interaction with phosphoinositides or other acidic lipids, leading to the creation of a substantial circular pore (52,53). This pore formation helps the release of IL-1β from the cells (54) GSDMD-mediated pyroptosis is key for cell death and host survival, and dysregulation may lead to cancer progression (55–57). However, apart from Caspase1, there is a second non-canonical pathway through Caspase 11, also upregulated by NLRP3 inflammasome upregulation that leads to cleavage of GSDMD and contributes to the downstream sequelae as described above (50,58). Initially limited to bacterial infections, Caspase-11-mediated pyroptosis has been associated with a variety of disease pathologies, such as lung injury and asthma, skin psoriasis, peptic ulcers in gastric tissue, and graft versus host disease (59–62). Recent studies with chronic stress-induced depression models have explored the role of canonical caspase-1-GSDMD pathway in neuroinflammation (63–65). However, the role of noncanonical activation by caspase-11 under psychosocial stress has not been explored yet.

In this study we investigate both canonical and non-canonical pathways of NLRP3 activation, and downstream effects on Il-1β release, and the effect of neuroinflammatory mediators as well as different behavioral endpoints related to anxiety, fear and working memory. Building on our work in mouse models with Ibrutinib, we further extend out

investigation into NLRP3 activation and Interleukin 1β in rats, which arguably have a wider repertoire of complex social behaviors that mice can exhibit and are a more advanced model of studying anxiety and cognitive behaviors. Additionally, from using just a physical model of stress accepted in the literature we also show that inducing psychological stress by exposing rats to a repeated social defeat paradigm produces a robust neuroinflammatory as well as neuronal phenotype with prominent behavioral deficits across many different domains. This allows us to get a closer approximation of human stress experience, as the social defeat paradigm is regarded as the most indicative animal model for investigating social stress (66). We then utilize known inhibitors of the molecules of the canonical and non-canonical pathways of NLRP3 inflammasome and GSDMD activation, alone and in combination on animals and demonstrate that a combination treatment approach offers the most efficacy to improve neural correlates, mitigate neuroinflammation and improve behavioural deficits in the model. Among the inhibitors we chose, the two major ones Ibrutinib and Disulfiram are both FDA approved for human use of either cancers or alcohol use disorder, thereby keeping our work relevant from a translational perspective (67–71). The key contribution of this paper is the contribution of the non canonical pathway post stress in several domains, from synaptic spine reductions, neuroinflammation to several dimensions of behavior. The second key result of this paper is the pharmacological inhibitor experiments that show that simultaneous inhibition of both the canonical and non canonical pathways downstream of NLRP3 inflammasome activation are more beneficial than employing either of the drugs alone.

Methods

Experimental animals

Male and female Sprague Dawley (SD) rats were obtained from National Institute of Biologicals, Noida, India and All India Institute of Medical Sciences, New Delhi, India. The rats were group housed in cohorts of 3 per cage with ad libitum access to rodent chow and filtered water. The rats were kept in vivarium under standard conditions (21 °C ± 2 °C temperature; 55% ± 10% humidity, 12 h:12 h light-dark cycle starting at 7 am; 20–22 lux light inside the cage; and corn cob bedding). Rats were acclimatized for at least two months before the start of the experiments. All animal experiments were conducted according to the guidelines and protocols approved by the Animal Ethics Committees of the Delhi University, India and MD University, Rohtak, India. Physiological parameters such as temperature, heart rate and body weight were monitored during the experiments. Experiments were initiated at the 5 months of age.

Pharmacological Inhibition of inflammasomes

Five-month-old SD rats were randomly assigned to control, and different drug treatment groups. Rats were administered with canonical and non-canonical inflammasome inhibitors or vehicles, starting at 5 h before the induction of stress, and again given at every 24 h for total 7 days. To pharmacologically inhibit caspase 11, wedelolactone dissolved in dimethyl sulfoxide (DMSO): polyethylene glycol 400 (PEG): water at 1:4:5 ratios were administered by oral gavage (30 mg/Kg/day; Sigma-Aldrich, St. Louis, MO), as reported earlier (72) Control rats were similarly dosed intragastrically (i.g.) with vehicle (DMSO: PEG). To inhibit GSDMD, rats were administered intraperitoneally (i.p.) with disulfiram (50 mg/Kg/day; Sigma-Aldrich) formulated in sesame oil (12.5 mg/ml), as reported earlier (68). Control animals were similarly dosed with vehicle (sesame oil, i.p.). To validate the observations

from disulfiram studies, another GSDMD inhibitor necrosulfonamide (Sigma-Aldrich) dissolved in DMSO was also used in a separate set of animals (20 mg/Kg/day, i.p.), as reported earlier (73). Control rats were similarly injected with vehicle (0.05% DMSO in saline). To pharmacologically inhibit NLRP3 inflammasome, a specific inhibitor MCC950 (50 mg/Kg/day, i.p.; Sigma-Aldrich) dissolved in DMSO was used, as we reported earlier (48). Control rats were injected with 0.05% DMSO in saline (i.p). To inhibit upstream pathway of NLRP3 inflammasome, a Bruton's tyrosine kinase (BTK) inhibitor ibrutinib (3 mg/Kg/day; i.p.; Sigma-Aldrich) dissolved in DMSO was used, as we reported earlier (48) .Control rats were injected in parallel with the vehicle (0.05% DMSO in saline) at the indicated times. To determine the effect of simultaneously inhibiting canonical and non-canonical inflammasomes, we administered MCC950 (50 mg/Kg/day; i.p.), a canonical NLRP3 inflammasome inhibitor, and wedelolactone (30 mg/Kg/day, i.g.), a non-canonical inflammasome inhibitor (caspase 11 inhibitor)(74). To determine the potential therapeutic efficacy of simultaneous inhibition of canonical and non-canonical inflammasome, we also used FDA approved inhibitors, ibrutinib (3 mg/Kg/day; i.p) and disulfiram (50 mg/Kg/day; i.p.).

Stress paradigms:

Stress has a profound effect on developing anxiety-like behavior. We used two types of stresses to induce anxiety-like behavior in 5-month-old SD rats. Rats were randomly assigned to control and stress conditions. Restraint stress followed by underwater submersion was used for physical stress paradigm. Repeated social defeat was used to induce psychosocial stress. Three weeks prior to behaviour experiments, rats for control and stress induction were handled daily at the testing arena to reduce the external anxiety. All the behavior procedures were conducted during the dark phase (7 pm and 11:30 pm) of the cycle to avoid potential

influence of day-time noise and disturbances. The stressed animals were singly housed to avoid the potential influence of social housing on the anxiogenesis.

Physical stress

Rats were subjected to physical stress-induced anxious behavior based on a method adapted from our earlier study (48). In brief, rats were transported out of colony room to stress room to induce physical stress. On the first day, rats were restrained by immobilizing them in perforated polycarbonate chambers (measuring 21 cm long x 9 cm wide x 7 cm high) for 3 hours. The restraining chamber was placed in the inclined plane of 75 degree with head positioned downward during the entire 3 hours of immobilization. Rats were then moved to solitary housing in a separate cage with food and water. Next day, rats were subjected to underwater trauma by first allowing them to swim for 45 s in a container filled with ice-cold water, and then suddenly pushing down to gently submerge them completely underwater for 30 s. Rats were again moved to solitary housing with food and water and housed there during the entire duration of the rest of the experimental procedures. The restraining chambers and water containers for underwater trauma were cleaned with 70% ethanol solution and completely dried between rats to eliminate any odour cues.

Psychosocial stress

Five-month-old dominant and aggressive male SD rats were identified and paired with females, with one male and one female in a cage. After a month, these dominant male rats were conditioned for heightened aggression, once per week for 45 days, to attack the intruder by removing the resident female for an hour and placing a new 4-month-old male or female rat as an intruder for 15 minutes. After analyzing the conditioning sessions, most aggressive and dominant male rats were selected for the experiments. To induce the psychosocial stress, 5-month-old male and female SD rats were used as intruder, the test subjects for anxiety

studies. One hour before the induction of psychosocial stress, resident female rat was removed from the cage containing aggressor male. A new intruder test rat was placed into the home cage of the aggressor male for 15 minutes. The aggressor rat displayed full repertoire of aggressive behavior such as sideway threats, aggressive pursuits and bites on the intruder, which showed defensive and submissive postures, as described earlier (75). To prevent further physical injury while allowing the sensory interaction to stimulate psychosocial threat of attack, the intruder was taken out and put into a small wire mesh cage (25 cm x 10 cm x 10 cm) and then placed back into the home cage of the aggressor. After having spent a total of 3 hours, the defeated intruder rat was taken out and moved to solitary housing and the aggressive rat was reunited with its female companion in the home cage. This intruder test rat was again subjected to repeated social defeat by new aggressor rats for the next two days. To avoid habituation, different aggressors were used every day to instil psychosocial stress into the intruder test rats. During the entire course of repeated social defeat, the physical health status of the intruding test rats were carefully monitored, and significantly wounded rats were removed from the study. Only 7% of the rats met the removal criterion. The control animals were simply handled in the colony room and kept with their companion resident rats.

Analysis of anxious behavior and working memory

Seven days after the induction of physical and psychosocial stress, the test rats were assessed for the anxiety-like behavior using open field test (OFT), light-dark test (LDT), elevated plus maze test (EPM) and social interaction tests. Working memory was analysed by Y-maze and novel object recognition (NOR) tests. We also tested fear acquisition, extinction and recall using afear conditioning paradigm. All trial sessions were video recorded, and by a researcher blinded to group status of the rats. Rat behavior and memory function assessment was performed between 7 pm and 11:30 pm during the dark phase of the light cycle when rats are most active, being nocturnal and to avoid disturbance from daytime activities. In between

every test animal and trials, all behavioural tools and apparatus were thoroughly cleansed and deodorized with 70% ethanol and dried to eliminate olfactory cues from other experimental animals. Four days before the onset of behavior assessment the animals were shifted to the behavior testing room for 2 hours and remained undisturbed in their home cage to enable them to acclimatize to the new environment. Behaviour tests were performed in following sequence:

Open field test (OFT)

Analysis of anxious behavior was performed using an open aired (without ceiling) box-shaped apparatus made of black polycarbonate sheets (length 80 cm x width 80 cm x height 60 cm). The open field test was conducted to analyse anxious behavior based on a method adapted from our earlier study (48). In brief, first test rat was placed at the corner and allowed to freely explore in empty opaque activity open field arena box for 5 minutes. The time spent in the central area (40 cm x 40 cm) was measured to assess anxiogenic behavior. The more time spend in 20 cm wide periphery (thigmotaxis) is interpreted with the severity of anxiety, higher the thigmotaxis higher the presence of anxiety in rodents. Stressed animals tend to avoid the central area of the open field arena (76).

Elevated plus maze test (EPM)

The elevated plus maze raised to 100 cm height was used to measure anxiety from the unsafe height. The plus-shaped platform made of polycarbonate comprised four arms (60 cm long, 15 cm wide), with two opposite set of arms enclosed by 30 cm heigh walls and two other arms remained open. The opposite arms with enclosed walls represented secure area, while other set of open arms without the walls represented unsafe area (48). The arms were brightly illuminated using 100-lux light. To test the anxiety like behaviour in rats, each rat was placed in central square area of the elevated plus maze and allowed to explore freely in all arms for 5

min. The percentage of time spent into the open arm (unsafe area) was determined to assess the anxious behaviour (77). The rat was considered inside the open arm when all four limbs entered inside the open arm. Lower time spent in the open arm was taken as an indicator of higher degree of anxiety in rats.

Light-dark test (LDT)

Light-dark test was used to examine the innate tendency of rats to avoid brightly lit area and move to the safety of dark area, especially during stress (78). The box-shaped apparatus consisting of two compartments (25 cm length x 25 cm wide x 45 cm height), one covered with black opaque polycarbonate sheets to serve as dark area and other with clear polycarbonate sheets to act as light area. The apparatus was divided into two equal size compartments by a barrier that contained open door (10 cm x 10 cm) to enable a test rat to freely escape from brighter area to the darker area for safety, especially when stressed. Rats were allowed to explore the light-dark apparatus for 10 min and relative time in dark area to light area was counted (48). A higher dark/light ratio reflected higher anxiety.

Three chamber social interaction test

Social impairment induced by anxious stress, negatively impact both males and females (79). The psychological stress-induced social impairment was analysed by utilizing the sociability and social preference tests. The three-chamber test apparatus was constructed using a polycarbonate box (length 120 cm x width 40 cm x height 40 cm), consisting of three chambers, a middle chamber that opened in both directions constructed using sliding clear polycarbonate windows. The two side chambers were closed other than the entry/exit opening from the middle chamber. First, the test rat was habituated by letting it explore the empty chamber with both entry exit windows of the middle chamber open for 10 min and then transferred to home cage. A new rat referred to as rat 1 of same age and gender as test rat, was placed into one of the side

chambers with partially closed transparent polycarbonate window for 10 minutes. Thereafter, for the sociability session, the test rat was placed into the middle chamber and allowed to freely explore for 10 min. Time spent by the test rat trying to sniff around and trying to enter the chamber with rat 1 versus the empty chamber on the other side was recorded. The sociability preference index was determined by dividing the time spent as described above by the test rat with rat 1 to the time spent with empty chamber. At the end of this session, the test rat was removed and placed in the home cage for 10 min. Meanwhile, a novel rat referred to as rat 2 of same age and gender was placed into the empty side of the camber. To determine the social preference to novel, the test rat was again placed back into the central chamber for another 10 min. The social preference time was calculated by dividing the time spent by test rat with novel rat (rat 2) to the time spent with familiar rat (rat 1). Both rats 1 and 2 were consistent with the sex of the test rat. The placement of familiar rat and novel rat was systemically altered between trials to eliminate any chamber bias.

Novel object recognition test (NOR)

To investigate working memory in anxious rats, novel object recognition test (NOR) was performed as previously described (80), with minor modifications. The test rat was first habituated with test apparatus consisting of a black polycarbonate box (length 80 cm x width 80 cm x height 60 cm) for 30 min. Thereafter, the test rat was removed and put back in its home cage for 20 min. Two identical plastic toys (same size, shape, colour and texture) were placed nearly 10 cm away from the diagonally opposite corners of the test chamber. In the first familiarization phase, test rat was allowed to freely explore the two identical objects for 10 min. At the end of this session, the test rat was again removed to its home cage. Meanwhile, one of the familiar test objects was replaced with non-identical novel object (different size, shape, colour and texture). In the novel object recognition test final phase, the test rat was allowed to explore for 5 min with two these non-identical (one familiar and another novel

object). The exploration time spent by rat with familiar and novel object was measured. The percentage exploratory preference to novel object was determined to evaluate the anxiety-induced working memory deficits.

Y-maze test

To assess the spatial working memory, we used Y-maze test to determine the number of entries to the novel unexplored arm, as previously described (81). The black polycarbonate Y-maze apparatus consisted of three identical arms projected in Y-shape (length 60 cm x width 15 cm x height 30 cm). Visual spatial cues were provided around the Y-maze by placing differently coloured papers and objects on the top side of walls and roof of behavioural testing room to help differentiate the relative position of the three arms of the Y-maze. In the first phase of the test, the entry to the one of the three arms was blocked with black polycarbonate removable door. In this phase, the test rat was placed at the start of the one of the open arms and allowed to explore for 15 min, which is considered as acquisition trial. Rats were allowed to familiarize themselves with these two open arms to acquire the spatial cues and differentially identify the arms. During the entire period of the acquisition trial, the entry to the novel arm remained closed. At the end of acquisition trial, the test rat was removed and placed in home cage for 30 min. During the test trial, the entry to the novel arm was freely allowed by completely removing the black polycarbonate door. Rats were allowed to explore all the three arms of the Y-maze for 15 min in this phase, referred to as recall trial. The number of entries to the novel arm by this test rat was counted as compared to the total entries in all the three arms. A normal unstressed rat preferably explores novel arm more as compared to the two familiarized arms, indicating its ability to recall previously visited arms. Anxiety is associated with impairment of spatial memory, and anxious rats falter in their preference to novel arm.

Fear conditioning tests

The Pavlovian fear conditioning tests were performed to assess fear memory, as previously described (82), with minor modifications. In brief, we measured fear acquisition, extinction and recall over three consecutive days using polycarbonate chambers (length 45 cm x width 24 cm x height 40 cm). The apparatus was equipped with a speaker with 3000 Hz tone amplified to 86 dB. The floor of the chamber was made of a stainless steel grid to provide deliver a foot shock (500-ms, 0.5 mA). A day before fear acquisition test trials, the rats were acclimatized to the fear conditioning apparatus by placing them for 30 minutes without any sound or foot shock. On the first day of the fear acquisition trial, the test rat was allowed to freely move in the test chamber for 5 min of habituation. Thereafter, the test rat was subjected to five fear conditioning trials for fear acquisition. Each conditioning trial for fear acquisition consisted of 20 sec tones from speaker (conditioned stimulus) and a foot shock (un-conditioned stimulus) in the last 2 sec of the culmination of sound. Freezing time, defined by absence if any visible movement except for respiration-related movement, was measured during the 20 sec of conditioned sound. Each trial was separated by 210 sec intervals. The test rat was moved back to home cage after the fear acquisition trial. On second day, the test rat was again placed in the fear conditioning chamber and allowed to habituate for 5 min, followed by 10 fear extinction trials of only conditioned stimulus alone, i.e. 20 sec of the tone without any foot shock. To determine fear extinction, freezing time was similarly recorded during these 20 secs of conditioning stimulus. Inter-trail period was of 210 sec, where no stimulus was provided. Then test rat was moved back to its home cage. On the third day, after 5 min of habituation, the test rat was subjected to 10 trials of fear recall by exposing it to only conditioned stimulus of 20 sec sound, without any foot shock. Inter-trial interval in fear recall trial was also 210 sec. Freezing behaviour was similarly recorded over these 10 fear-cued recall trials. Percent

freezing time (sec spent freezing/20 sec conditioned stimulus) during fear acquisition, extinction and recall were calculated for stressed and control rats.

Tissue collection

Serial blood samples to analyse the corticosterone levels at various time points before and after the induction of stress were collected from the jugular vein, as previously described (83). In brief, a catheter was inserted into the right jugular vein of the rats and connected to a polyethylene tubing (PE-50) with heparinized saline (0.9% NaCl, 25 IU/ml). Blood samples of 150 µl were withdrawn using a syringe and centrifuged at 2000 g for 30 min at 4°C to collect plasma. Samples were stored in -80°C until ELISA. Eleven-days after the induction of stress, rats were anesthetized by ketamine (80 mg/Kg) and xylazine (10 mg/Kg). First, 150 µl of cerebrospinal fluid (CSF) was carefully collected from the cisterna magna, while avoiding the contamination from blood, as described earlier (Pegg et al. 2010). Thereafter, about 3 ml of blood was collected directly from the cardiac puncture and centrifuged to collect the plasma. The rats were transcardially perfused with 200 ml of ice-cold phosphate buffered saline (PBS) to maximally clear blood from the brain vasculature. The brains were quickly removed and various regions of brain like hippocampus, amygdala and prefrontal cortex were carefully isolated under the stereomicroscope and immediately stored in -80°C freezer for later use.

Golgi-Cox staining for dendritic spines

Golgi-cox staining was performed to analyse the apical dendritic spine density and number of mushroom shape spines in CA3 region of hippocampus in both stressed and unstressed rats. Golgi-cox method consist of various steps, which includes specimen impregnation with Golgi-cox solution, cryoprotection, sectioning, colour development and mounting as described earlier (84,85), with minor modifications. In brief, rat brains were isolated and

impregnated in dark with Golgi-cox solution containing potassium dichromate, mercuric chloride and potassium chromate for 40 days at room temperature. To preserve tissue morphology brains were transferred into cryoprotection solution containing 20% sucrose and 15% glycerol in water for 3 days. Coronal rat brain sections of thickness 100 µm were cut using a vibratome (VT1200S, Leica, Nussloch, Germany). Thereafter, sections were mounted on chrome alum-gelatinized slides. In colour development step, slides were washed with double-distilled water and then incubated in 75% ammonia solution for 10 min in dark. Sections were washed with water and fixed by treatment with 1 % sodium thiosulphate solution for 10 min. The brain sections were dehydrated with ethyl alcohol series (70%, 90% and 100%) and cleared in xylene. Subsequently, sections were mounted using Permount mounting medium, and slides were kept in dark until microscopic examination. To visualize dendritic spines, brightfield images with frame size of 1024x1024 pixels were captured using 100x objective with 1.3 numerical aperture and BX63 Olympus microscope (Olympus Corporation, Tokyo, Japan). Five different sections from each rat were used to determine the mean spine density and mean number of mushroom spines per 10 µm of apical dendrite in the CA3 region of the hippocampus. The dendrites directly emerging from the primary shaft from soma were classified as primary apical dendrites, as described earlier (86) . Dendritic spines from CA3 region were categorized and counted with open-source software ImageJ (National Institute of Mental Health, Bethesda, MD). Mushroom spines were classified by their shape of mushroom, with head diameter greater than 0.5 µm and head-to-neck ratio greater than 1:1. The number of spines were counted by experimenter blinded to the identity of the samples.

Isolation and culture of peripheral blood mononuclear cells

Rat peripheral blood mononuclear cells (PBMC) were isolated from the 3 ml of heparinized blood collected through cardiac puncture. The separation and isolation of PBMC from rats

was performed by density gradient centrifugation using OptiPrep solution (Sigma-Aldrich), as we described earlier (48). In brief, OptiPrep density gradient solution of iodixanol in water (60% w/v) was layered with diluted blood in buffered saline (0.85% NaCl, 10 mM Hepes, pH 7.4) and centrifuged at 400 g for 30 minutes at 20°C. PBMC were carefully collected from a sharp band at the interface and washed twice with tricine-buffered saline. The cells were pelleted by centrifugation (200 g, 15 minutes at 20°C). The purity of PBMC, determined morphologically by May-Grünwald Giemsa (MGG) staining, was nearly 99%. To culture, PBMCs were resuspended in RPMI 1640 medium (Sigma-Aldrich) supplemented with 10% fetal calf serum (Hyclone, Logan, UT). PBMC were cultured to the concentration of 2.5×10^6 cells/ml and a set of these cells were primed with LPS from *Escherichia coli* serotype 0111: B4 (100 ng/ml) and nigericin (10 µM). The control and primed cells were treated with various inhibitors for inflammasomes, such as wedelolactone (40 µM), MCC950 (5 µM), ibrutinib (1 µM), disulfiram (100 nM), or 0.2% DMSO as vehicle control. The cell culture supernatant and cells were collected and kept at -80°C for later use.

Cell viability assay

The viability of PBMCs were determined using WST-8 assay, as described earlier (87). Briefly, non-toxic 2-(2-methoxy-4-nitrophenyl)-3-(4-nitrophenyl)-5-(2,4-disulfophenyl)-2H-tetrazolium monosodium salt (WST-8) (Dojindo Molecular Technologies, Gaithersburg, ML) was added to the control and LPS-primed PBMCs, and cells treated with inhibitors. PBMCs were incubated for an hour to allow cells to metabolize WST-8 to form a water-insoluble formazan product, which is detected by absorbance at 460 nm. The absorbance of WST formazan at 460 nm is directly proportional to the cell viability.

Cell permeabilization assay

SYTOX green was used to measure cell permeabilization, as described previously (88). SYTOX green is a low molecular weight (<0.6 kDa) DNA binding fluorescent dye that infiltrate into the cells following the plasma membrane pore formation, an indicator of cell pyroptosis. SYTOX green is not permeable to undamaged cells. SYTOX green fluorescent intensity increases more than 500-fold following binding with DNA, and thus onset of pyroptosis can be more sensitively detected based on its uptake. PBMCs were treated with vehicle, LPS and inhibitors as indicated earlier. To quantify cell permeabilization cells were treated with 2.5 mM SYTOX green (Sigma-Aldrich) and cells were kept in CO_2 incubator. To determine cell permeabilization, fluorescence at 528 nM after excitation at 485 nM was recorded using Biotek Synergy plate reader (Agilent, Santa Clara, CA).

Immunoblot analysis

The rat brain tissue samples and PBMCs were analysed for the protein levels of Gasdermin D N-terminal fragment, cleaved caspase 11, NLRP3, cleaved caspase 1 and β-actin by immunoblotting, as we described earlier (48,89). In brief, brain tissue samples and PBMCs were homogenized in RIPA lysis buffer with protease and phosphatase inhibitor cocktails (Thermo Fisher Scientific, Waltham, MA) using sonicator (Mesonix Sonicator 3000, Cole-Parmer, Vernon Hills, IL). These homogenates were centrifuged at 14,000 g for 25 min at 4°C and then protein content was measured by BCA protein assay kit (Thermo Fisher Scientific). Equal protein samples were prepared in Laemmli sample buffer and separated by SDS PAGE electrophoresis (Bio-Rad Laboratories, Hercules, CA) on 4-12% Tris-glycine gels (4-12%). The proteins were transferred onto the PVDF membrane (Bio-Rad Laboratories) and blocked with 5% bovine serum albumin (IgG-free endoprotease-free BSA, Jackson ImmunoResearch Laboratories, West Grove, PA) in 50 mM Tris–HCl (pH 7.4), 150 mM NaCl and 0.1% Tween

20 (Tris-buffered saline with Tween-20, TBST). The PVDF membranes were incubated for overnight at 4°C with following primary antibodies: anti-cleaved gasdermin D (Asp276, rabbit monoclonal antibody, 1:1000, #10137, Cell Signaling Technology, Danvers, MA); anti-cleaved caspase 11 p20 (mouse monoclonal antibody, 1:1000, #50-256-3377, Fisher Scientific, Waltham, MA); anti-NLRP3 (D4D8T, rabbit monoclonal antibody, 1:1000, #15101, Cell Signaling Technology); anti-cleaved Caspase 1 (p20, Asp296, E2G2I, rabbit monoclonal antibody, 1: 1000, #89332, Cell Signaling Technology), β-actin (mouse monoclonal antibody, 1:10000, #sc-47778, Santa Cruz Biotech, Dallas, TX). The membranes were washed five times with TBST and incubated for 1 h at room temperature with horseradish peroxidase-conjugated goat-anti rabbit IgG secondary antibody (1:10,000, #STAR124P, Bio-Rad Laboratories) or horseradish peroxidase-conjugated goat anti-mouse IgG (1:10,000, #sc-2005, Santa Cruz Biotech). Membranes were washed again with TBST, and protein bands were detected using SuperSignal West Pico PLUS Chemiluminescent substrate (Thermo Fisher Scientific).

Quantitative real-time PCR

The hippocampal samples from experimental rats were used to determine the mRNA levels of C-C motif chemokine ligand (CCL2), CC chemokine receptor 2 (CCR2) and 18S as a housekeeping gene by quantitative reverse transcription polymerase chain reaction (qRT-PCR). The total RNA was extracted from the hippocampal samples was extracted by RNeasy kit and treated with DNase (Qiagen, Germantown, MD) following manufacturer's instructions. The concentration of RNA preparation was assessed at 260 nm. Samples with absorbance ratios of 260/280 and 260/230 greater than 1.7 were used for used for qRT-PCR. RNA samples were reverse transcribed by using SuperScript III reverse transcriptase (200U) and poli-T primer (0.1 μg, Invitrogen, Carlsbad, CA). The target cDNA was amplified using HotStart-IT SYBR Green qPCR master mix (USB, Cleveland, OH) and RT-PCR system

(Applied Biosystem, Foster City, CA). Following oligonucleotide primers were used CCL2 F-AGCCAACTCTCACTGAAGC, CCL2 R-GTGAATGAGTAGCAGCAGGT, CCR2 F-CACCGTATGACTATGATGATG, CCR2 R-CAGGAGAGCAGGTCAGAGAT, 18S F-AGTCGCCGTGCCTACCAT and 18S R-GCCTGCTGCCTTCCTTG. The relative mRNA levels were calculated using comparative threshold cycle CT (ΔΔCT) method, as described previously (90).

Caspase 1 activity assay

Caspase 1 enzymatic activity in rat brain samples and PBMC was assessed using a caspase 1 colorimetric assay kit based on spectrophotometric detection of chromophore p-nitroaniline (p-NA) after cleavage from substrate YVAD-pNA, as per manufacturer's instructions (YVAD, Merck Millipore, Burlington, MA). In brief, the brain tissue and PBMC were homogenized in ice-cold lysis buffer and mixed with 2.5 nM dithiothreitol and 50 µl caspase 1 reaction buffer in a 96-well flat bottom microplate. A substrate solution containing YVAD-pNA was added to each well, followed by incubation at 37°C for 2 h. The enzymatic activity of caspase 1 was measured at 405 nm using an ELISA plate reader (Molecular Devices, San Jose, CA).

Enzyme-linked immunosorbent assays (ELISA)

The rat brain, plasma, CSF and PBMC samples were used to assess the levels of corticosterone, IL1β, Gasdermin D, C-X-C motif chemokine ligand 2 (CXCL2) and intracellular adhesion molecule-1 (ICAM1) using commercially available enzyme-linked immunosorbent assays (ELISA) kits, as per manufacturers' instructions. In brief, the plasma levels of corticosterone were measured by DetectX corticosterone ELISA kits (#K014-H1, Arbor Assays, Ann Arbor, MI). IL1β levels in rat brain, plasma and PBMC were quantified by IL1beta Quantikine ELISA kits (#RLB00, R&D Systems Inc, Minneapolis, MN).

Gasdermin levels in the rat brain CSF was measured by GSDMD ELISA kits (#orb1784611, Biorbyt, Durham, NC). Rat hippocampal samples were used to assess the levels of CXCL2 using CXCL2/CINC-2 Quantikine ELISA kit (#RCN300, R&D Systems Inc). ICAM1 levels in rat hippocampus was measured by using ICAM1/CD54 Quantikine ELISA kit (#RIC100, R&D Systems Inc).

Statistical analysis

For statistical analysis, the open-source program JAMOVI (The Jamovi project 2022, Version 2.3) was utilized. Most of our data needed different factorial ANOVA designs, which are mentioned in relevant result sections below. Throughout, the main and interaction effects in all ANOVAs have been reported along with their partial eta square (ηp2) in order to indicate effect sizes. When interaction terms were significant, we broke it down with post-hoc testing, else significant main effects were tested for group differences. To keep the paper readable, we have only reported the significant interaction terms in the main text for the multiple ANOVAs conducted. We have broken down significant interactions using simple main effects analysis. For ANOVAs that needed more complex design beyond a 2X2 factorial style, the most complex significant interaction term has been analysed post-hoc for pairwise comparison. Animal numbers for each experiment are mentioned in the text and/ or legends for individual figures. For all ANOVAs, significant interaction terms have been analysed using Bonferroni-corrected post hoc test. A detailed narrative results section for all statistical analysis is included in the supplementary files and page numbers have been referenced wherever necessary. For each post hoc comparison, t values have been reported in the text alongside p values instead of Cohen's d as measures of effect size because Cohen's d in JAMOVI is not adjusted for multiple comparisons. The significance threshold has been set at $p < 0.05$ for all analyses.

Results

Both physical and psychological stress models elicit a robust behavioral and neuroinflammatory phenotype in rats, more aggressive in females:

We established two different paradigms of stress, one physical and one psychosocial, in 5 months old Sprague Dawley rats. The model and the day wise protocol are shown in Figure 1A and narrated in detail in the methods section. Both physical and psychosocial stress elicited a robust upregulation of IL-1β in plasma, as measured by an ELISA assay. Our previous experience in mouse models of stress had shown us that female rodents typically display a more aggressive phenotype post stress, both in behavioral and neuroimmune endpoints. Plots indicated a similar pattern to data in the rat models as well. We conducted a 2X2 ANOVA to assess the effects of stress type and sex on plasma IL-1β levels (ng/ml) 10 days post-stress (Figure 1B) . The analysis revealed a significant main effect for stress type, [$F(2, 64) = 66.30$, $p < 0.001$, $\eta p^2 = 0.674$], a significant main effect for sex [$F(1, 64) = 21.83$, $p < 0.001$, $\eta p^2 = 0.254$], and also a significant interaction between stress type and sex [$F(2, 64) = 6.31$, $p = 0.003$, $\eta p^2 = 0.165$]. Post hoc pairwise comparisons with Bonferroni correction were conducted thereafter which showed significant differences in plasma IL-1β levels based on stress type and sex. In the Control group, no significant difference was observed between female and male rats (M difference = −0.41, SE = 2.00, $t(64) = -0.205$, $p = 1.000$). However, in the Physical Stress condition, females exhibited significantly higher IL-1β levels than males (M difference = 8.62, SE = 2.00, $t(64) = 4.30$, $p < 0.001$), and both females (M difference = −19.60, SE = 2.05, $t(64) = -9.58$, $p < 0.001$) and males (M difference = −10.57, SE = 1.96, $t(64) = -5.40$, $p < 0.001$) had higher levels compared to the Control group. Similarly, in the Psychosocial Stress condition, females had significantly higher IL-1β levels than males (M difference = 7.88, SE = 1.96, $t(64) = 4.02$, $p = 0.002$), and both females (M difference = −16.99, SE = 2.00, $t(64) = -8.48$, $p < 0.001$) and males (M

difference = −8.69, SE = 1.96, t(64) = −4.44, $p < 0.001$) had higher levels compared to the Control group. No significant differences were observed between the Physical Stress and Psychosocial Stress conditions for either females (M difference = 2.61, SE = 2.00, t(64) = 1.31, p = 1.000) or males (M difference = 1.88, SE = 1.96, t(64) = 0.96, p = 1.000).

Next, we investigated IL-1β levels in three areas of the brain that are implicated in anxiety, depression and stress in literature, the Hippocampus, the amygdala and the prefrontal cortex (Figure 1C). The results were analyzed by three separate 2X2 ANOVAs with stress condition (control, stress) and sex (males, females) as factors. While control levels of IL-1β in all three areas of the brain stayed consistent and similar in male and female rats, in each brain area, both psychosocial and physical stress elevated IL-1β. This upregulation was more robust in hippocampus and amygdala and especially in females In the hippocampus the ANOVA revealed a significant interaction effect between stress type and sex [$F(2, 64) = 9.53$, $p < 0.001$, $\eta p^2 = 0.229$] and more IL-1β in females in the physical stress model (compared to stressed males, M difference = 146.08, SE = 26.5, t(64) = 5.51, $p < 0.001$) as well as in the psychosocial stress model (compared to stressed males, M difference = 141.86, SE = 25.9, t(64) = 5.47, $p < 0.001$). Similar observations were found in the amygdala, with a significant interaction between stress and sex [$F(2, 64) = 7.71$, $p < 0.001$, $\eta p^2 = 0.194$], and a more robust upregulation in females both in physical (compared to stressed males, M difference = 120.9, SE = 30.9, t(64) = 3.91, p = 0.003) and psychosocial stress (compared to stressed males, M difference = 184.0, SE = 30.2, t(64) = 6.09, $p < 0.001$) models. In both hippocampus and amygdala there were large and very significant differences between control as well as stressed conditions. Individual mean differences and p values are noted in the supplementary results section (Pg. 2-3, Supplementary materials) and in Figure 1C. In the Prefrontal Cortex stress conditions did lead to elevated IL-1β levels but to a lesser extent than limbic structures [$F(2, 64) = 14.54$, $p < .001$, $\eta p^2 = 0.312$] but not sex and the interaction term

was not significant. IL-1β rose in animals undergoing physical stress compared to control animals (Females: M difference = −147.9, SE = 36.0, t(64) = −4.11, p = 0.002; Males: M difference = -100.9, SE = 34.5, t(64) = −2.93, p = 0.071), as well as Psychosocial stress, but only in females (M difference = −135.2, SE = 35.2, t(64) = −3.84, p = 0.004). Notably there was no significant difference in the upregulation of IL-1β between the two models, except in PFC, as was the case in plasma and CSF. Analysis of IL-1β in the CSF also showed similar trends and significant upregulation of IL-1β in both models of physical stress (Figure 1D). Additionally, we also characterized the elevation of cortisol in control and stressed animals in both models of stress (Figures S1A and S1B) every 8 hours for 24 hours and then every 24 hrs. till 96 hours post stress. These were analyzed with a 2X2X8 mixed factorial ANOVA with stress, sex and time as factors. Stressed females consistently displayed elevated cortisol from males, and stressed animals overall displayed peaks in plasma cortisol consistent with extant literature. A complete narrative result of the statistical results may be found in the supplementary results section (pg.81-82).

Next, we characterized the behavioral phenotype in our models of stress (Figures 1E-1H. We utilized tests of anxious behavior well validated in rodents that we have utilized before i.e. The Elevated Plus Maze (EPM) tests, Open Field Test (OFT) and the Light-Dark test (LDT). We also utilized two tests of working memory which is reported to suffer in stress, viz. the Novel Object Recognition (NOR) and Y-maze tests. The methods section outlines our setup and detailed protocols for each of these tests. In the light dark test (LDT) the rats were placed in a chamber with a well lit clear half with an opening to the dark half of the chamber for 5 minute. The ratio of time spent in the dark versus the light half of the test chamber (D/L ratio) provides a measure of the rat's anxiety. The higher this ratio, the higher is the level of anxiety in the animal. In control animals the time is roughly equal with animals exhibiting a marginal preference for the dark half, which is statistically not significant. The results in Figure 1E

show that both stress models led to elevated D/L ratio in animals subjected to physical and psychosocial stress. The ratio was particularly high in female animals in both models of stress. Statistically a 2 (Male, Female) X 3 (Control, Physical Stress, Psychosocial Stress) factorial ANOVA demonstrated significant main effects of stress type [$F(2, 64) = 62.00$, $p < 0.001$, $\eta p^2 = 0.660$] and sex [$F(1, 64) = 55.20$, $p < 0.001$, $\eta p^2 = 0.463$], as well as a significant interaction between stress and sex [$F(2, 64) = 15.00$, $p < 0.001$, $\eta p^2 = 0.319$] which was broken down by simple main effects analysis. Under Physical Stress, females had a significantly higher D/L ratio compared to males (M difference = −1.99, SE = 0.33, $t(64) = -6.02$, $p < 0.001$). Additionally, females exhibited a significantly higher D/L ratio compared to the Control group (M difference = −3.31, SE = 0.34, $t(64) = -9.79$, $p < 0.001$), and males also showed an increased D/L ratio compared to the Control group (M difference = −1.26, SE = 0.32, $t(64) = -3.90$, $p = 0.003$). Under Psychosocial Stress, females also exhibited a higher D/L ratio compared to males (M difference = −2.29, SE = 0.32, $t(64) = -7.07$, $p < 0.001$). Additionally, females exhibited a significantly higher D/L ratio compared to the Control group (M difference = −3.38, SE = 0.33, $t(64) = -10.22$, $p < 0.001$), while males also showed a increased D/L ratio compared to the Control group (M difference = −1.04, SE = 0.32, $t(64) = -3.21$, $p = 0.031$). the males and females in the control group showed no difference in their D/L ratios.

This pattern was repeated with similar effect sizes and post hoc t scores in Open Field Test (OFT; Figure 1E). Briefly, this test quantifies the patterns of movements by rats in an open arena, and the measure utilized is the time spent in the demarcated central part of the arena. Anxious mice demonstrate less time spent in the central arena and spend more time trying to find an escape route along the periphery of the arena, whereas control animals have a random pattern of exploring the arena with no preference exhibited for a specific part. This difference in clearly reflected in our data. In both models of stress, physical and psychosocial, the time

spent in the central arena fell sharply and the decline was more pronounced and significant in females. The trends in the Elevated Plus Maze test (EPM) were also similar (Figure 2D). In this test, the rats are placed in the center of a plexiglass plus shaped apparatus that stands around 100cm tall from the floor, which is a considerable height for rats, who have an innate dislike for heights. Two arms of the plus are walled, and the other two arms are open. When put at the center of the maze and allowed to explore it for around 5 minutes, naïve rats display a preference for spending more time in the closed vs open arms. However, anxiety is associated with a further sharp decline in the time spent in open arms and a proportional increase in the time that rats spend hiding inside the closed arm. Our results faithfully replicated this pattern (Figure 2G). In both models of stress, the time spent in the open arm of the EPM fell, and females showed a more robust decline that males did.

Next we investigated working memory in stressed vs. control rats. We performed a Y Maze test as the first assessment tool for working memory, where we first let the rat explore the Y shaped testing apparatus with one arm of the Y blocked. During the trial the block was removed, and the rat was placed in the maze, free to explore in any direction. Control rats usually display preference for the newly unblocked arm of the Y to explore it more, as they remember the existing arm from the habituation phase. However, stress is usually associated with an abolishment of this preference and by extension, an impairment in working memory. This is what our data also revealed (Figure 1G). Both physical and psychosocial stress were associated with a fall in percent entry into the novel arm compared to controls. Statistical analysis with a 2X3 Factorial ANOVA as described above revealed significant main effects of stress and sex type but also a significant interaction [$F(2, 64) = 3.21$, $p = 0.047$, $\eta p^2 = 0.091$] which was further analyzed by a simple main effect analysis. Both physical stress and psychosocial stress led to a reduction in open arm entry, however, interestingly this difference was more pronounced in male animals, for physical stress (Compared to controls: (M

difference = 19.96, SE = 3.68, $t(64) = 5.418$, $p < 0.001$; Compared to stressed females: M difference = 12.05, SE = 3.77, $t(64) = 3.20$, $p = 0.032$). In the Psychosocial Stress condition, both females (M difference = 13.87, SE = 3.77, $t(64) = 3.68$, $p = 0.007$) and males (M difference = 18.62, SE = 3.68, $t(64) = 5.05$, $p < 0.001$) showed significantly lower entries compared to the Control group. We validated these results with the Novel Object Recognition (NOR) task, which is also a well-accepted behavioral test for working memory in rodents. In this test, rats are exposed to an object (usually a small toy) in a fixed location in an arena. After a short time, they are reintroduced into the arena but with a second novel object. Animals with their working memory intact display a preference for the novel object by spending more time around it, sniffing and poking it with their snouts. A fall in this preference marked by the time they spend around the novel object is taken as a mark of decline in working memory. Or results showed a pattern similar to the Y maze test (figure 1H). Control rats, both male and female preferentially spent time with the novel object. However, time spent with the novel object declined in stressed animals, signified by an interaction between stress and sex [$F(2, 64) = 13.4$, $p < .001$, $\eta p^2 = 0.295$]. This test also replicated the phenomenon of males showing more deficit in working memory compared to females when stressed. Under the Physical Stress condition, males spent significantly less percent time with the novel object compared to the Control group (M difference = 16.66, SE = 2.44, $t(64) = 6.83$, $p < 0.001$), while females showed no significant difference (M difference = 1.84, SE = 2.55, $t(64) = 0.72$, $p = 1.000$). Similarly, in the Psychosocial Stress condition, males spent significantly less percent time with the novel object compared to the Control group (M difference = 14.65, SE = 2.44, $t (64) = 6.01$, $p < 0.001$), but females again showed no significant difference (M difference = −1.82, SE = 2.49, $t(64) = -0.73$, $p = 1.000$).

Notably, in the behavioral tests as well as in IL-1β levels in the plasma, brain areas and the CSF, both stress models did not significantly differ in their ability to elicit a phenotype. The

detailed narrative reporting of all statistical tests for Figure 1 panels can be found on the supplementary results section (Pg 1-9).

Both Psychosocial and Physical Stress models display a robust upregulation of the non-canonical mediators of the NLRP3 inflammasome pathway, more pronounced in female animals.

We next investigated the levels of the known non-canonical mediators of the NLRP3 inflammasome pathway, viz. Gasdermin D (GSDMD), Caspase 1 and Caspase 11. Hippocampal lysates from psychosocially stressed rats probed with relevant antibodies demonstrated upregulated GSDMD N terminal, which is produced by a cleavage of GSDMD by Caspase 1 and/ or Caspase 11 (Figure 2A) 10 days post stress. Blots also showed cleaved caspase 11 prominent upregulation of NLRP3 and p20 fragment of cleaved Caspases 1 and 11, suggesting their activation. All of the bands appeared most intense in female stressed rats. Relative densitometry measurement of band intensities normalized against β-Actin confirmed significantly increased band intensities for GSDMD N terminal (Figure 2B), p20 fragment of cleaved Caspase 11 (Figure 2C), NLRP3 (Figure 2D) and p20 fragment of cleaved Caspase 1 (Figure S1C), in the hippocampal lysates of rats subjected to psychosocial stress compared to controls, particularly in females. Data were analyzed by a 2 (Stress, control) X 2 (Male, Female) ANOVA. We also checked if the protein level of GSDMD rose following stress in both models with an ELISA assay. In line with our prediction, both physical and psychosocial stress resulted in increased amount of GSDMD in CSF, and this increase was more prominent in female rats (Figure 2E). We further investigated Caspase 1 Enzyme activity in both hippocampus and amygdala of rats under both physical (Figure S1F) and psychosocial stress (Figure 2F). Under both conditions Caspase 1 activity rose in both Hippocampus and Amygdala, with female animals showing higher levels in both groups compared to control

rats (Figure 2F and Figure S1F). In control rats there were no male/female difference in either GSDMD levels or Caspase 1 activity between male and female rats.

We also calculated Pearson's correlation coefficients between the rats' performance on two behavioral assays, namely the Percent time spent in the open arms of the EPM (Figure 2G) and the time spent in the central part of the OFT arena (Figure 1F) with the GSDMD levels in the CSF measured with an ELISA. CSF GSDMD values correlated negatively with percent time spent in the open arms of the EPM in both males ($r = –0.650$, $p = 0.022$, $df = 10$) and females ($r = –0.682$, $p = 0.021$, $df = 9$) under physical stress (Figure 2H) . Under the psychosocial stress condition as well, there was a significant negative correlation between CSF GSDMD levels and the percent time spent in the open arm of the EPM in both males ($r = –0.715$, $p = 0.009$, $df =10$) and females ($r = –0.6797$, $p = 0.015$, $df =10$; Figure 2I). We also calculated correlations between CSF levels of GSDMD and time spent in the central square of the OFT arena (Figure S1D-E). The analysis revealed a significant negative correlation between open arm time and Gasdermin D levels in CSF in males ($r = –0.694$, $p = 0.012$, $df = 10$) and females ($r = –0.633$, $p = 0.037$, $df = 9$) under physical stress (Figure S1D). Similarly, under psychosocial stress (Figure S1E), we also found significant negative correlations between CSF GSDMD levels and the time spent in the central square of the OFT arena in males ($r = –0.708$, $p = 0.010$, $df = 10$) and females ($r = –0.663$, $p = 0.019$, $df = 10$). The correlation data suggested that elevated GSDMD levels in the CSF correlated with higher degree of anxious behavior in both our stress models. A detailed narrative statistical report of all panels in figure 2 can be found in the supplementary results section (Pg 9-17).

Until this point we have provided a thorough behavioral characterization of both stress models we developed, using both neuroimmune (systemic and brain) and behavioral (anxiety, working memory) readouts. We also established how the non-canonical mediators of the NLRP3 inflammasome pathway and the NLRP3 molecule itself are upregulated in both stress

models and showed that enhanced levels GSDMD in CSF is associated with higher anxiety. Notably, in none of our endpoints, we saw any significant differences between the physical stress and the psychosocial stress models. The psychosocial stress model which used a repeated social defeat paradigm produced an equally strong neuroimmune and behavioral phenotype post stress. Because the psychosocial stress paradigm is conceptually closer to psychological stress experienced by humans, we conducted the next series of pharmacological experiments in the model of psychosocial stress. Henceforth we refer to this as "stress" for the rest of this paper.

Pharmacological inhibition of Caspase 11 by Wedelolactone reduces neuroinflammation, improves anxiety, working and fear memory, and enhances fear extinction and extinction recall.

We utilized a naturally occurring botanical, Wedelolactone to suppress Caspase 11 in this experiment, as described in literature. Figure 3A shows the design of the experiment with drug dosage, route of administration and the timeline. Detailed protocols have been described in the methods section. We measured IL-1β in hippocampal lysates with an ELISA assay (Figure 3B). a 2 (Control, Stress) X 2 (Male, Female) X 2 (Vehicle, Drug) factorial ANOVA was utilized to analyze the results. The results showed significant main effects for stress, sex, and drug treatment on hippocampal IL-1β levels. Additionally, significant two-way interactions were observed between stress and sex [$F(1, 74) = 22.79$, $p < 0.001$, $\eta p^2 = 0.235$] and between stress and drug [$F(1, 74) = 29.29$, $p < 0.001$, $\eta p^2 = 0.284$]. The interactions between Stress and Drug and the three-way interaction term was not significant. Simple main effect analysis on the two significant interaction terms were conducted. Post hoc pairwise comparisons with Bonferroni correction for stress and sex factors showed that under the Psychosocial Stress condition, females exhibited significantly higher IL-1β levels compared to the Control group (M difference = −335.84, SE = 22.9, $t(74) = -14.70$, $p < 0.001$), as did

males (M difference = −181.58 SE = 22.9, $t(74) = -7.95$, $p < 0.001$). Comparisons between sexes within the Psychosocial Stress condition revealed that females had significantly higher IL-1β levels than males (M difference = 156.91, SE = 22.0, $t(74) = 7.14$, $p < 0.001$). Bonferroni corrected pairwise comparisons for stress and drug treatment revealed no significant difference between vehicle- and wedelolactone-treated groups in the Control condition (M difference = –22.9, SE = 23.7, $t(74) = -0.97$, $p = 1.000$). Under the Psychosocial Stress condition, vehicle-treated animals exhibited significantly higher IL-1β levels compared to the Control group (M difference = −346.2, SE = 23.2, $t(74) = -14.94$, $p < 0.001$). Similarly, wedelolactone-treated animals under Psychosocial Stress also showed higher IL-1β levels compared to the Control group (M difference = −171.3, SE = 22.5, $t(74) = -7.60$, $p < 0.001$). Within the Psychosocial Stress condition, however, animals treated with wedelolactone had significantly lower IL-1β levels compared to vehicle-treated animals (M difference = 152.0, SE = 22.0, $t(74) = 6.92$, $p < 0.001$). A very similar pattern was observed in Il-1β measured in lysates from the amygdala (Figure S2A) and CSF levels of IL-1β assayed with ELISA (Figure 3C). Once again, Wedelolactone reduced the levels of IL-1β elevated in stressed animals compared to vehicle treated animals, both the elevation and the pharmacological effect greater in females. Similar trends were found in Caspase 1 activity assays in lysates from the hippocampus (Figure 3D) and the amygdala (figure S2B). GSDMD levels in CSF also followed the same pattern: Wedelolactone brought down the GSDMD levels in stressed rats compared to vehicle treated rats (Figure S2C). We then proceeded to measure behavioral outcomes following inhibition of Caspase 11 in stressed and control rats with wedelolactone vs vehicle treatment. In measures of anxious behavior viz. LDT (Figure 3E), OFT (Figure 3F) we saw the same pattern of heightened anxiety in stressed rats, particularly in females, and this was significantly mitigated in wedelolactone treated females compared to vehicle treated rats. The effect sizes and pairwise mean differences are reported

in the supplementary results (Pg. 19-23). Working memory was assessed with the Y Maze test (Figure 3G) and Novel Object Recognition task (Figure S2D). Once again, the same patterns were seen in stressed vs control animals as were shown in Figures 1 and S1. Working memory deficits were seen in stressed animals, however, more in males than females. This was significantly mitigated by Wedelolactone treatment. The main effects, interactions, effect sizes and post hoc mean differences are narrated in the supplementary results (Pg. 23-24 and 90-91).

Next, we also ran a fear conditioning paradigm on these animals to test different aspects of fear memory (Figures 3H and 3I). Animals were conditioned on day 1 (Day8 of the timeline in Figure 3A), and extinction and extinction recall were tested on the second and the third consecutive days (Days 9 and 10 of the timelines shown in Figure 3A) respectively. A detailed protocol has been shared in the methods section. Briefly, the animals acquired a fear of a sound presented for 20 seconds within the fear conditioning chamber, over repeated trial blocks, coupled to a brief 0.5mA foots hock delivered through the metal floor grid, lasting through 500ms anytime within the last 2 seconds of the sound playing. Percent time they spent freezing was measured as a measure of fear acquisition. All rats acquired fear within 3-5 trials but in the vehicle treated stressed animals, both males and females displayed a higher rate of freezing (Figures 3H and 3I). Wedelolactone treatment significantly reduced percent freezing responses in stressed animals. Through both days of testing extinction and extinction recall, when the sound was presented to the rats without the noxious foot shock stimulus, wedelolactone treated animals demonstrated reduced freezing in both males and females. We analyzed this data with a 2(stress, control) X 2 (drug, vehicle) X 3 (Time) Mixed factorial ANOVA with 3 of the trials for each day, as marked with p values in Figures 3H and 3I. The detailed main effects, interactions and effect sizes with post-hoc comparisons with mean differences across trials are reported in supplementary results (Pg. 24-33). However, even

from the plots in figures 3H and 3I graphed with mean and 95% CIs, on the acquisition day vehicle treated stressed animals started displaying mean freezing responses with non-overlapping CIs from the 3rd trial onwards from all other groups, including the wedelolactone treated stressed rats, both male and female. Likewise, on days 9 and 10 when extinction and recall were being tested, the vehicle treated stressed rats continued to display higher freezing responses with CIs that do not overlap with any other groups for most of the trials in both males and females but the traces in female rats show a better separation. Taken together, this data suggests wedelolactone treatment suppresses GSDMD cleavage by reducing Caspase11 and in turn lowers IL-1β and improves behavioral outcomes in general.

Pharmacological inhibition of GSDMD cleavage by Disulfiram reduces neuroinflammation and improves behavioral outcomes in stressed rats compared to controls

We used a second inhibitor (Disulfiram) of the non-canonical inflammasome pathway to allosterically inhibit GSDMD cleavage by Caspases 1 and 11. Disulfiram is an FDA approve drug which is widely used in treating alcohol use disorder. The experimental timeline and treatment regimen, route of administration and design are shown in Figure 4A. Plasma, area specific brain lysates and CSF of Vehicle and drug treated control, and stressed rats were then assessed for levels of IL-1β with ELISA assays (Figures 4B-D). The data were analyzed with 2 (stress, control) X Drug (Disulfiram, Vehicle) X Sex (Male, Female) factorial ANOVA. In plasma, IL-1β was elevated as before with stress, more pronounced in females in vehicle treated rats. Disulfiram treatment did not alter levels of IL-1β in the plasma in control animals, however, reduced them significantly in stressed rats, compared to vehicle treated groups (Figure 4B). However, the treatment did not mitigate the elevated IL-1β levels entirely comparable to control levels. Similar results were obtained for IL-1β levels in hippocampus and amygdala (Figure 4C) and the CSF. To validate our results with Disulfiram and confirm

that these findings came from inhibition of GSDMD cleavage, we also treated a third group of rats with Necrosulfonamide, a potent inhibitor of this cleavage (73). Treatment with necrosulfonamide also reduced IL-1β in the CSF, in a pattern like Disulfiram (Figure 4D; Pg 33-38). When we tested these animals for behavioral endpoints, the Disulfiram treated rats displayed statistically significant reductions in anxiety. Exemplar traces from the OFT arena shows a marked absence of central square crossing in vehicle treated stressed female rats, compared to controls (Figure 4E). Stressed female rats treated with Disulfiram show some restoration in central square crossings. This is reflected in quantification of the data in Figure 4F. The data were analyzed with a 2X2X2 Factorial ANOVA as described above. Apart from main effects, significant two-way interactions were observed between stress and sex [$F(1, 84) = 9.61$, $p = .003$, $\eta p^2 = 0.103$] and between stress and drug [$F(1, 84) = 20.39$, $p < .001$, $\eta p^2 = 0.195$]. Post hoc pairwise comparisons with Bonferroni correction for stress and sex factors revealed that under the Psychosocial Stress condition, females spent significantly less time in the central arena compared to the Control group (M difference = 23.58, SE = 2.66, $t(84) = 8.87$, $p < .001$), as did males (M difference = 11.92, SE = 2.66, $t(84) = 4.49$, $p < .001$). Comparisons between sexes within the Psychosocial Stress condition revealed that females spent significantly less time in the central arena than males (M difference = –13.79, SE = 2.60, $t(84) = –5.31$, $p < .001$). Post hoc comparisons with Bonferroni correction for stress and drug treatment revealed no significant difference between disulfiram- and vehicle-treated groups in the Control condition (M difference = −2.68, SE = 2.72, $t(84) = −0.99$, $p = 1.000$). Under the Psychosocial Stress condition, vehicle-treated animals spent significantly less time in the central arena compared to the Control group (M difference = 26.23, SE = 2.66, $t(84) = 9.87$, $p < .001$), as did disulfiram-treated animals (M difference = 9.26, SE = 2.66, $t(84) = 3.48$, $p = .005$). Within the Psychosocial Stress condition, however, disulfiram-treated animals spent significantly more time in the central arena compared to vehicle-treated

animals (M difference = 14.29, SE = 2.60, $t(84) = 5.50$, $p < .001$) The necrosulfonamide treated group of rats also showed the same pattern of reduction of anxious behavior in stressed animals compared to vehicle treated ones. Similar results were obtained in LDT (Figure 4G). Y maze test results repeated the stress induced reduction in working memory, more prominent in males which improved significantly in both disulfiram and necrosulfonamide treated animals vs vehicle treated rats subjected to psychosocial stress (Figure 4H).

A combination treatment with pharmacological inhibitors of both the canonical and non-canonical mediators of the inflammasome pathways offer better behavioral rescue and more robust amelioration of neuroinflammation in stressed versus control rats

Earlier, we have shown how a BTK inhibitor, Ibrutinib, which is also FDA approved for treating certain kinds of human cancers, can improve stress induced anxious behavior in mice. For the next phase of our experiments in rats, we employed a combination therapy approach, using two sets of drugs, comparing them to individual drug treated groups and vehicle treated groups. We used two separate sets of drugs and parallel experiments. The drugs, dosages, administration routes and timeline of drug administration, induction of stress and assessment are all outlined in Figure 5A. For the first set of experiments, we wanted to obtain proof of concept data that inhibition of the NLRP3 inflammasome and Caspase 11 will be beneficial both by reducing neuroinflammation and anxiety. To that end we treated animals with MCC950, a well-known selective inhibitor of NLRP3 inflammasome assembly and Wedelolactone which as described above, reduces Caspase11, individually, and in combination on separate groups of rats alongside vehicle treated rats. The combination treated group demonstrated lower IL-1β levels in the hippocampus not only relative to the vehicle treated stressed animals but also compared to the individual drug treated groups (Figure 5B). Specifically, in the hippocampus, a significant interaction between drug

treatment and psychosocial stress was observed [$F(3, 76) = 32.8$, $p < .001$, $\eta p^2 = 0.564$]. Notably, comparisons between treatment groups under the psychosocial stress condition revealed that animals treated with MCC950 + Wedelolactone had significantly lower IL-1β levels compared to animals treated with either only Wedelolactone (M difference = −154.82, SE = 31.2, $t(76) = -4.96$, $p < 0.001$) or only MCC950 (M difference = −212.92, SE = 31.2, $t(76) = -6.82$, $p < 0.001$). Working memory assessment with the Y maze task echoed the exact same pattern in female rats. Vehicle treated rats displayed a worsening under stress, and although individual treatments with either MCC950 or Wedelolactone alone was less efficacious than the combination treatment (Figure 5C). Aside from the main effects the 2X2 factorial ANOVA revealed a significant interaction between drug treatment and psychosocial stress [$F(3, 76) = 11.8$, $p < .001$, $\eta p^2 = 0.317$]. Again, comparisons within the psychosocial stress condition revealed that animals treated with MCC950 + Wedelolactone exhibited significantly higher percentages of entries compared to animals treated with MCC950 (M difference = 13.12, SE = 2.94, $t(76) = 4.47$, $p < .001$). This suggests that a combination treatment approach of blocking NLRP3 inflammasome assembly with reducing Caspase 11, a part of the non-canonical mediator of the NLRP3 inflammasome assembly produces a more robust benefit than using them in isolation.

The second set of experiments combined Ibrutinib, an FDA approved inhibitor of BTK, a canonical mediator of NLRP3 inflammasome assembly. Previously we have shown that Ibrutinib treatment improves stress-induced anxiety and reduces neuroinflammatory mediators in mice. For this set of experiments we wanted to try inhibiting both the canonical and non-canonical pathways of NLRP3 inflammasome activation by employing Ibrutinib (that inhibits the canonical pathway) and Disulfiram (an inhibitor of the non-canonical pathway by the way of blocking GSDMD cleavage). To this end, we treated groups of rats with Ibrutinib and Disulfiram alone and in combination, and compared them to vehicle

treated rats under stress and control conditions, as shown in Figure 5A. We also added a new behavioral readout assay, the Social Preference test , as shown in Figure 5C. Briefly, for this test, the experimental rat is placed in the central chamber of the apparatus as shown. After a brief habituation period when the rat is free to explore the entire three part chamber, one clear plexiglass window is partially closed and a rat (Rat 1, same biological sex as the experimental rat) is placed in the side chamber, and the behavior and time the rat spends trying to interact with Rat 1 is scored. Through the open window the experimental animal can smell Rat 1 in the side chamber. In the second phase of the test a novel rat (Rat 2, same biological sex as the experimental rat) is placed in the second side chamber and again the behavior and time the experimental rat spends to approach Rat2 is scored. Two indices can be calculated from this test as shown in Figures E and F. Sociability (Figure 5E) refers to the sociability preference index determined by dividing the time spent by the test rat with rat 1 to the time spent with empty chamber. Social Preference (Figure 5F) is calculated by dividing the time spent by test rat with novel rat (rat 2) to the time spent with familiar rat (rat 1).

Both sociability and social preference deteriorates drastically with stress in vehicle treated animals (Figures 5E-F). A 2 (Control, Stress) X 2 (Male, Female) X 4 (Vehicle, Ibrutinib, Disulfiram, Combination treatment) factorial ANOVA revealed significant two-way interactions between stress and sex [$F(1, 152) = 15.32$, $p < .001$, $\eta p^2 = 0.092$] and between stress and drug [$F(3, 152) = 33.83$, $p < .001$, $\eta p^2 = 0.400$], apart from main effects of all 3 for sociability (Figure 5E). The interaction was further broken down by a simple main effects analysis. The general worsening was more prominent in females across all treatment groups. Post hoc pairwise comparisons with Bonferroni correction for stress and drug factors revealed that animals under psychosocial stress treated with Vehicle exhibited significantly lower sociability scores compared to those treated with Disulfiram (M difference = 0.347, SE = 0.0501, $t(152) = 6.93$, $p < .001$), Ibrutinib (M difference = 0.279, SE = 0.0501, $t(152) = 5.57$,

$p < .001$), and Disulfiram + Ibrutinib (M difference = 0.8404, SE = 0.0501, $t(152) = 16.78$, $p < .001$). However, animals treated with both Disulfiram + Ibrutinib under psychosocial stress had significantly higher Preference Index scores compared to those treated with only Disulfiram (M difference = 0.494, SE = 0.0501, $t(152) = 9.85$, $p < .001$) or only Ibrutinib (M difference = 0.561, SE = 0.0501, $t(152) = 11.21$, $p = < .001$). Similar results were obtained for Social Preference for the novel rat (Rat2) as well (Figure 5F).

Next, we investigated synaptic spine parameters in CA3 hippocampal neurons of these rats in Golgi-Cox stained thick sections. Spine counts, density and specifically mushroom spine morphologies have been associated with learning ability (91,92). Both animal and human studies of depression, anxiety and stress have demonstrated neuroplastic changes in terms of spine density and morphology(93–95). Consistent with this, in our hands, we saw significant reduction of spine density in 20 µm long dendrite segments of CA3 hippocampal neurons (5 sections/ per animal) in vehicle treated female rats subjected to stress, compared to controls (Figure 5G and 5H). A 2X2X4 factorial ANOVA as designed above showed A two-way factorial ANOVA revealed significant main effects for psychosocial stress and drug treatment on the number of dendritic spines per 10 µm in female rats. Additionally, a significant interaction between psychosocial stress and drug treatment was observed [$F(3, 76) = 3.01$, $p = 0.035$, $\eta p^2 = 0.106$]. Post hoc pairwise comparisons with Bonferroni correction for psychosocial stress and drug treatment factors revealed that stressed animals treated with Disulfiram + Ibrutinib also showed significantly higher spine density compared to vehicle-treated animals (M difference = 2.727, SE = 0.650, $t(76) = 4.20$, $p = 0.002$). However, animals treated with vehicle under psychosocial stress did not show significantly different spine density compared to only Disulfiram-treated animals (M difference = 2.091, SE = 0.650, $t(76) = 3.22$, $p = 0.053$), nor only Ibrutinib-treated animals (M difference = 1.127, SE = 0.650, $t(76) = 1.734$, $p = 1.000$).

Next we quantified the number of mushroom spines, in the dendritic segments of CA3 hippocampal neurons (associated with better memory performance in cognitive tasks (92) in female animals subjected to stress vs. controls, across all 4 treatment groups (Figure 5I). A 2X2X4 Factorial ANOVA showed main effects of stress and drug, qualified by a significant interaction [$F(3, 76) = 13.7$, $p < 0.001$, $\eta p^2 = 0.351$]. As clear from Figure 5G and the trend in Figure 5I, stress caused a sharp reduction of mushroom spines in dendrites. Although not a full rescue, Post hoc pairwise comparisons with Bonferroni correction for psychosocial stress and drug treatment factors revealed that under the psychosocial stress condition, animals treated with Disulfiram + Ibrutinib had significantly higher mushroom spine percentages compared to vehicle-treated animals (M difference = 10.835, SE = 1.12, $t(76) = 9.66$, $p < 0.001$). Again, within the psychosocial stress condition, animals treated with Disulfiram + Ibrutinib exhibited significantly higher mushroom spine percentages compared to animals treated with only Disulfiram (M difference = 3.914, SE = 1.12, $t(76) = 3.49$, $p = 0.023$) or only Ibrutinib (M difference = 5.574, SE = 1.12, $t(76) = 4.97$, $p < 0.001$).

We also studied other mediators known to drive IL-1β driven neuroinflammatory responses under neurodegeneration, stress and injury : CCL2, CXCL2 and ICAM1 (96). CCL2 and CCR2 are a microglial chemokine and its cognate monocytic receptor pair, expressed by glial cells, brain endothelial cells and neurons, which serve as important chemoattracts for immune cells to the brain. CCL2-CCR2 ligand-receptor binding is essential for microglia mediated monocyte recruitment to the brain endothelium(97,98). In the repeated social defeat paradigm we utilized in our psychosocial stress, an upregulation of both is noted in the literature (99,100). Consistent with this, in our hands, in female vehicle treated rats under stress, both CCL2 and CCR2 mRNA displayed a marked elevation (Figures 5J and 5K). The combination treatment seems to be able to mitigate this elevation better than the individual drugs alone. A 2X2X4 factorial ANOVA for CCR2 mRNA levels showed main effects for

both drug and stress with a significant interaction between them [$F(3, 75) = 25.9$, $p < 0.001$, $\eta p^2 = 0.509$]. When broken down, post hoc pairwise comparisons with Bonferroni correction for psychosocial stress and drug treatment factors revealed that under the psychosocial stress condition, animals treated with Disulfiram + Ibrutinib exhibited significantly lower fold change levels compared to vehicle-treated animals (M difference = −1.9879, SE = 0.154, $t(75) = -12.95$, $p < 0.001$). Stressed animals treated with Disulfiram + Ibrutinib also had significantly lower fold change levels compared to those treated with either Disulfiram alone (M difference = −0.8352, SE = 0.154, $t(75) = -5.44$, $p < .001$) or Ibrutinib alone (M difference = −1.1243, SE = 0.154, $t(75) = -7.32$, $p < .001$). Very similar results were obtained with CCL2 mRNA (Figure 5I). In addition, we also probed for two other markers of neuroinflammation. ICAM1, an adhesion molecule expressed by endothelial and immune cells whose upregulation is associated with increased inflammation and in models of social defeat (99–103) was elevated post stress in hippocampal lysates from vehicle treated rats, the elevation rescued slightly by individual treatment with Ibrutinib or Disulfiram, and to a greater extent by the combination treatment. Similar trends were also observed in CXCL2, another chemokine associated with exacerbated NLRP3 mediated neuroinflammation (104–106) In case of both these mediators, the combination treatment was better at checking stress induced elevations that the two drugs employed by themselves (Figure S3A, B).

Taken together, the data in figure 5 suggested that a combination treatment approach works better, when the canonical and non-canonical pathways of NLRP3 inflammasome activation are targeted simultaneously. We got orthogonal validation of this from neural endpoints, neuroinflammatory mediators of interest as well as behavioral data. We therefore conducted our final set of pharmacological inhibition experiments using a combination treatment of Disulfiram and Ibrutinib.

A combination of Disulfiram and Ibrutinib leads to improved behavioral endpoints and reduced neuroinflammatory responses in stressed versus control rats

The design and timeline of the experiment is shown in Figure 6A along with drug dosages and routes of administration. Combination treatment reduced IL-1β in lysates from the hippocampus and amygdala (Figure 6B) plasma (Figure S4A) and CSF (Figure S4B), otherwise starkly increased in vehicle treated stressed rats. The elevation of IL-1β and its mitigation by the combination treatment is sharper in female rats. A 2 (Stress, Control) X 2 (Male, Female) X 2 (Vehicle, Combination treatment) factorial ANOVA revealed significant main effects for drug treatment, stress and on Hippocampal IL-β levels with significant two-way interactions were observed between drug treatment and stress [$F(1, 82) = 54.47$, $p < .001$, $\eta p^2 = 0.399$] and between stress and sex [$F(1, 82) = 17.25$, $p < .001$, $\eta p^2 = 0.174$]. Post hoc pairwise comparisons with Bonferroni correction showed that in the vehicle group, animals under psychosocial stress exhibited significantly higher IL-1β levels compared to the control group (M difference = −390.9, SE = 24.3, $t(82) = -16.07$, $p < .001$). Comparisons between treatment groups under psychosocial stress revealed that animals treated with Ibrutinib + Disulfiram exhibited significantly lower IL-1β levels compared to those treated with Vehicle (M difference = −236.2, SE = 23.2, $t(82) = -10.18$, $p < .001$). Similar results were seen in amygdala, plasma and CSF for IL-1β. We found the same trend in Caspase 1 activity data in both the hippocampus and the amygdala (Figure 6C).

We next assessed fear memory in the animals. We found very similar patterns in the data as we had found in Wedelolactone treated animals. Vehicle treated animals under stress showed higher freezing rates during fear acquisition on Day 8, with females showing more freezing (Figures 6D-E). When tested on Day 9 for extinction, and Day 10 for recall, vehicle treated stressed rats persistently showed higher freezing responses even though they did demonstrate extinction eventually. Notably, the traces for both female and male rats under stress that

received the vehicle stayed distinctively apart from the rest of the traces for all other groups with minimum overlap of 95%CI bars throughout the trials. This separation is even more prominent for females, suggesting a significant difference across all timepoints tested. In contrast, the combination treatment group is almost indistinct from the control group traces. The mixed factorial ANOVA results reflecting this summary are described in the supplementary results section (Pg 59-68).

The behavioral tests for anxiety (LDT and OFT) and working memory (Y-Maze and NOR) also showed significant improvements in the combination therapy group, with vehicle treated animals doing predictably worse (Figures 6F-H). Once again, we observed a worse deficit in male animals as clearly seen in Figure 6H in working memory tasks like Novel Object Recognition, where the trace around the novel object is distinctly different in vehicle treated animals under stress, and the bulk of the movement trace shows the animal just navigating the periphery of the arena (lower bottom panel, Figure 6H). The combination therapy restores the rats movement around the two objects. The quantitative data in Figures 6I and 6J also recapitulate this finding. Detailed narrative results from these ANOVAs are described in supplementary results (Pg 68-72).

Mechanistic experiments in cell culture studies demonstrate pyroptosis as a mechanism underlying propagation of inflammation in stressed rats

In extant literature the activation of NLRP3 inflammasome and Caspase 1 leads to cleavage of GSDMD into its N Terminal. The cleaved fragment auto-oligomerizes to form pores in the cell membrane through which cytosolic molecules start leaking into the extracellular space (39). We conducted a set of in-vitro mechanistic experiments using PBMCs purified from rats under control and stress conditions, from various drug treated groups and expanded in cultures to verify if this was the case in these animals. Our prior work in mice has also shown

that the activation of NLRP3 inflammasome pathway under conditions of stress is quite prominent in peripheral monocytes. PBMCs purified from control versus stressed animals show darker bands on Western Blots for GSDMD N terminal and cleaved Caspase 11. Even within the isolated cells, the increase was more apparent in cells from female rats under stress (Figure 7A). Relative densitometry of GSDMD N Terminal and the cleaved p20 fragment of Caspase 11 band intensities (Figures 7B-C) reflect this trend.

Next, we treated cultures of PBMCs isolated from control and stressed rats, treated with drugs as shown (Figure 7D) with either vehicle or Lipopolysaccharide (LPS), a biochemical component of the bacterial cell walls and known elicitor of inflammatory response. Naïve/vehicle treated PBMC cultures from both vehicle and wedelolactone treated animals show baseline elevated levels of IL-1β to begin with. However, when challenged with LPS, there is a massive upregulation of IL-1β in the PBMC cultures. Notably, PBMC cultures originating from Wedelolactone treated rats, which arguably had lower levels of NLRP3 activation via a reduction in Caspase 11 and therefore a subdued non canonical pathway) the elevation of IL-1β in response to LPS is also significantly less. From here onwards, we only show data from LPS challenged PBMC cultures originating from female animals which have a more robust neuroinflammatory phenotype as seen above repeatedly.

In the next series of in-vitro experiments we compared the levels of IL-1β and caspase 1 activity in PBMC cultures originating from control or stressed females treated with different drugs alone or in combination (Figure 7E-G). When PBMC cultures originating from female rats under control or stress condition treated with vehicle, MCC950, Wedelolactone or a combination of both were challenged with LPS, IL-1β levels increased in the culture media across all groups, yet with differences consistent with in vivo experiments and our hypotheses for the in-vitro experiments. While all cultures originating from drug treated animals mitigated the rise in IL-1β upon the LPS challenge, MCC950 and wedelolactone combination

treated animals provided cultures that were most resistant to this rise compared to either MCC950 or wedelolactone alone. Predictably the mitigation was more extensive in cultures that came from control rather than stressed rats, across all drug treatment groups (Figure 7E). Naïve cultures of PBS from control and stressed animals also displayed similar findings without any LPS challenge (Figure S5C). Although PBMC cultures from stressed female rats secreted higher amount of IL-1β in the culture media, this was mitigated somewhat in cultures that originated from animals treated with Ibrutinib, Disulfiram or both. The mitigation was most prominent in the cultures that came from animals receiving the combination treatment. We repeated the LPS challenge experiment with cultures originating from animals treated with vehicle, Ibrutinib, Disulfiram or both (Figure 7F). Once again, the rise in IL-1β in the culture media from the LPS challenge was most extreme in PBMC cultures from vehicle treated animals, and considerably higher in cultures from stressed animals. Again, each drug on its own mitigated this elevation, more efficiently in cultures from control animals. But the cultures from the combination treated animals, regardless of whether they came from stressed or control rats, were most resistant to the LPS challenge induced upshot of IL-1β. The result of probing for Caspase 1 activity in the culture media (Figure 7G) reflected the same pattern as Figure 7F. Together, the data from Figures 7D-G provided us with an invitro cellular model where we could further perform mechanistic investigations. Since we wanted to investigate whether the membrane of the cells is riddled with small pores (enabling pyroptosis to occur) we did a time course assay with Sytox green, a dye that usually does not permeate across intact cell membranes (88). As seen in Figure 7H, the cultures originating from control animals do not take up the dye well at all, regardless of their origin in animals with or without wedelolactone. However, LPS challenged cultures that originate from stressed animals (red trace) steadily take up the dye over 180 minutes, supporting the existence of pores in the cell membrane. LPS challenged cultures from

stressed rats treated with wedelolactone however, take up the dye slower and to a lesser extent (green trace). This suggests that the cells originating from animals with even one inhibitor of NLRP3 inflammasome activation mitigates the leakage partially when challenged with LPS. We repeated this experiment with PBMC cultures from the other set of drug treated animals (Figure 7I). In this experiment, we included naïve PBMC cultures unchallenged with LPS, originating from control rats as a baseline (blue trace). All the other traces are from LPS challenged PBMC cultures originating from stressed rats that were treated with vehicle, Ibrutinib, Disulfiram or both. Once again, the trace from LPS treated cells originating from vehicle treated stressed rats show the most uptake of Sytox green that almost appear sigmoid in shape. Ibrutinib and Disulfiram are individually able to slow down the uptake and mitigate it, but together they are much better at reducing Sytox green uptake (green trace). The p values from the mixed factorial ANOVA are mentioned on the traces of figures 7H and 7I. We also checked whether this leaky membrane led to lytic cell death. To this end, we performed WST8 viability assays (87) on all of the cultures (Figure S5A, D). However, there is no evidence of a decline in cell viabilities between any of the groups as shown. The full results of the statistical analysis for all panels in Figures 7 and S5 can be found in the supplementary results section (Pg. 72-82 and Pg.95-99, respectively). We did not see any evidence of cell death by LDH assays (data not shown). Taken together the experiments in PBMCs suggested that these cells are in a pyroptotic state, with a leaky membrane, possibly driving the neuroinflammatory cycle by releasing IL-1β which can initiate transcription of more NLRP3 as well as its own mRNA in other cells once released.

Discussion

In this study we built upon the foundation of our early work in mice, when we had provided rigorous evidence of the upregulation the BTK-NLRP3-Caspase-1 pathway induced in models of psychological stress (predator odor) and physical restrain stress. We had also

shown that treatment with Ibrutinib, an FDA approved drug for treating certain human cancers mitigates the neuroinflammation , particularly reducing IL-1β and rescues anxious behaviours in mice under the stressed condition (48). We extend these findings in this study and take up a parallel cleavage of GSDMD by Caspase 1, which facilitates pyroptotic release of IL-1β as discussed in the introduction of this paper. We also investigate the non-canonical pathway of GSDMD cleavage, that is associated with NLRP3 inflammasome activation and mediated by Caspase 11, not Caspase 1. Interestingly, Caspase 1 can process both Pro-IL1β to IL-1β as well as cleave GSDMD to its N and C terminals (51,107,108), but Caspase11 has no known substrate other than GSDMD (109,110). Parallel to our earlier results, several other groups have published results that confirm that the canonical Caspase-1-GSDMD pathway is involved in neuroinflammatory responses underlying chronic stress induced depression as well as a range of other inflammatory diseases (63–65,111–113). The GSDMD/Caspase 11 pathway has been studied in other disorders as discussed in the introduction, but the role of non-canonical activation mediated by caspase 11 has not been studied in models of psychosocial stress or psychological disorders well. We designed most of the experiments in this study to fill this gap. Conceptually the literature that exists suggesting both canonical and non-canonical pathways contribute to drive the IL-1β response suggested that stopping one pathway alone would not mitigate the IL-1β response under stress. We therefore hypothesized that a combination of drugs blocking both canonical and non-canonical pathways that ultimately prevented both cleavage of Pro-IL1β to IL-1β and GSDMD to its N and C terminals would be a better strategy.

We have provided first evidence in our knowledge about the role of both canonical and non canonical activation in psychosocial stress. We also provide detailed characterization of the rat model of chronic social defeat adapted from existing literature, but with an added step of housing rats in solitary cages post stress episodes. There is evidence that solitary housing

influences corticosterone levels and sleep duration, so we hypothesized this may also elicit a more robust stress response (114). While characterizing the neuroinflammatory response in stressed animals we also report robust elevation of IL-1β not only in the brain structures and plasma as other studies have reported, but also in the CSF, which is consistent with observation in human patients of depression and anxiety (106,115–117) but is being reported in an animal model of psychological stress for the first time. With elevated neuroinflammation, we also replicate the behavioral trends of impairment we observed earlier with mice. Female rats show a more pronounced phenotype for anxiety and fear memory as well as neuroinflammation, which is also consistent with human data. Interestingly we also observed that working memory deterioration was worse in male rats. For fear memory, we did not run a statistical comparison between males and females given the already complex ANOVA designs of our experiments but once again females did seem to have a more robust phenotype. In general an elevation of IL-1β is associated with impaired learning and memory *in vivo* (118–120) but we know the neuroimmune response to any kind of injury , stress or even neurodegeneration is not identical between the sexes in animal studies (121,122). Moreover, working memory involves frontal areas of the brain that are distinct from hippocampus-amygdala circuits that are mostly recognized for their role in fear and anxiety. It is quite plausible that there is some sex specific plasticity that is selectively different in these brain areas that underlies the males showing more deficits in working memory vs the females displaying more anxiety.

The second half of where this study contributes to extant literature is in the pharmacological experiments we have conducted. We have provided robust evidence that inhibiting Caspase11 and GSDMD cleavage using Wedelolactone and Disulfiram respectively mitigates functional impairments and attenuates neuroinflammation. We then show that both the FDA approved inhibitors we work with, Ibrutinib and Disulfiram, are less efficacious alone than in

combination to mitigate not only behavioral dysfunction and neuroinflammation, but also to improve neuronal spine density reductions that psychosocial stress seems to exacerbate. This is also a novel finding to our knowledge in an animal model of psychosocial stress. This is robust proof of concept pre-clinical evidence that argues for considering these inhibitors as novel therapeutic candidates to be used in conjunction with traditional pharmacotherapies for common psychological illnesses associated with stress, anxiety and depression. Our findings are also consistent with recent studies with Disulfiram that has shown anxiolysis in mice(123). Since Disulfiram is routinely used by clinicians to treat alcohol abuse disorder because of its ability to inhibit Alcohol Dehydrogenase (ALDH), these authors also used a second ALDH inhibitor, Cynamide, on their mouse model but that did not have any anxiolytic effect. This also supports indirectly our claim that the reduction in anxious behavior we see from Disulfiram treatment is a result of inhibition of GSDMD cleavage rather than its ALDH inhibiting properties.

We also developed a cellular assay for us to isolate PBMCs from stressed versus animals, and thereafter challenging them with LPS to emulate stress. Using cells from animals treated with different drugs we were able to demonstrate a mechanism of leaky cells, consistent with the concept of pyroptosis that the GSDMD literature also suggests and arrive at a model displayed in Figure 7J. We hope that this comprehensive set of experiments will form a stepping stone for further human studies investigating these pathways in stress, depression and anxiety.

Figure Legends

Figure 1. Molecular and Behavioural Characterization of the rat models of physical and psychosocial stress. **(A)** 5 months old male and female Sprague-Dawley (SD) rats were used for physical and psychosocial stress models. To elicit physical stress, restraining stress for 3 hours was performed on the first day followed by underwater trauma for 30 seconds on the next day. For psychosocial stress, animals were subjected to thesocial defeat paradigm for 3 consecutive days with different aggressor rats of same biological sex. Behavioral analysis was performed after one week of stress induction and all the animals were sacrificed and samples collected after 11 days of stress induction. IL1β levels in plasma (**B**), brain homogenates (**C**), and CSF (**D**) was measured with ELISA. Significantly higher level of IL1β was observed in plasma, CSF, hippocampus and amygdala of stressed rats, and females showed markedly higher IL1β as compared to males. Light-dark test (**E**) and open field test (**F**) were performed to assess anxious behavior. Female rats exhibited significantly pronounced anxiety levels after stress and than their male counterparts, as evident by their reluctance to spend time in light chamber (higher dark-light ratio) of light-dark test, and their hesitation to explore the central area of open field test. Y-maze test (**G**) and novel object recognition (**H**) was performed to assess working memory. Physical stress significantly enhanced the working memory deficits in male rats as compared to females, as depicted by their significantly lower entries to novel arm in Y-maze, and lesser time spent with novel object in the novel object recognition test. All data are presented as mean with 95% CI (n=10-12); p values are indicated for specific pairwise comparisons.

Figure 2. Psychosocial stress induces both canonical and non-canonical NLRP3 inflammasome pathway. (A) Immunoblotting was performed to measure protein expressions of gasdermin D-N terminal, cleaved caspase 11, NLRP3, cleaved caspase 1 and β-actin from hippocampal homogenates of male and female rats with (+) or without (-) psychosocial stress. Densitometric analysis showed significantly higher levels of gasdermin D-N terminal **(B)**, cleaved caspase 11 **(C)**, NLRP3 **(D)** under psychosocial stress. Gasdermin D levels **(E)** in the CSF was assessed ELISA assay and caspase 1 activity measured by activity assay kit **(F)**. Higher levels of cleaved caspase 1 and NLRP3 levels

under psychosocial stress indicated induction of canonical inflammasome pathway in brain. Enhanced levels of cleaved caspase 11 and gasdermin D-N terminal suggest activation of non-canonical inflammasome pathway in brain, which was significantly higher in females than male counterparts. Elevated plus maze **(G)** was performed to assess anxiety-like behaviors. Female rats under physical and psychosocial stress showed heightened anxiety-like behavior than their male counterparts, as they spent significantly less time in open arms of the elevated maze. Elevated plus maze scores and gasdermin D levels in CSF under physical stress **(H)** and psychosocial stress **(I)** were subjected to Pearson correlation analysis. Both male and female rats have shown moderate to high negative correlation with gasdermin D levels in CSF and to time spent in open arms (less time in open arms represents more anxiety). All data are presented as mean with 95% CI (n=10-12); p values are indicated for specific pairwise comparisons.

Figure 3. Wedelolactone attenuates IL1β and behavioral dysfunction in rats with psychosocial stress. (A) SD rats subjected to repeated social defeat-induced psychosocial stress were dosed with wedelolactone, a caspase 11 inhibitor, or vehicle for 7 consecutive days, starting from the first day of stress induction. IL1β levels in hippocampal homogenates **(B)** and CSF **(C)** were measured by ELISA assay. Wedelolactone treatment significantly reduced the IL1β levels in rats with psychosocial stress. IL1β is processed by activated caspase 1, and to examine its activity after wedelolactone treatment we performed caspase 1 activity assay **(D)**. Wedelolactone treatment significantly inhibited caspase 1 activity in rats subjected to psychosocial stress. We have performed light-dark test **(E)** and open field test **(F)** to evaluate anxiety-like behavior following wedelolactone treatment. Wedelolactone treated rats spent significantly more time in light chamber of the light-dark test and in the central area in open field test than vehicle stressed group, suggesting its anxiolytic effect. Wedelolactone treatment also improved working memory, as evident by significantly higher preference for novel arms than vehicle group in Y-maze test **(G)**. Anxiety is associated with heightened fear memory responses such as enhanced fear acquisition, extinction and recall. To determine the fear memory response, fear acquisition, extinction and recalls experiments were performed over 3 days in male **(H)** and female rats **(I)**. Wedelolactone treatment significantly attenuated the fear memory responses in male and

female stressed rats. All data are presented as mean with 95% CI (n=10-12); p values are indicated for specific pairwise comparisons.

Figure 4. Disulfiram, a gasdermin D inhibitor, suppresses IL1β and anxious behavior following repeated social defeat. (A) SD rats subjected to repeated social defeat-induced psychosocial stress received disulfiram or vehicle for 7 consecutive days started from the first day of stress induction. IL1β levels in plasma **(B)**, hippocampal and amygdala homogenates **(C)** and CSF **(D)** were measured by ELISA assay. Disulfiram treatment significantly reduced the IL1β levels in rats subjected to repeated social defeat. To validate the observations from disulfiram studies, another gasdermin D inhibitor necrosulfonamide was used **(D)**. Necrosulfonamide treatment significantly reduced IL1β levels following psychosocial stress, suggesting gasdermin D contribution in induction of IL1β levels in brain. To evaluate the effect of disulfiram treatment on anxiety-like behavior, in open field test **(E-F)** and light-dark test **(G)** were performed. Animals with anxiety prefer to stay close to the walls of open field than the central open area of the box during open field test. Disulfiram and necrosulfonamide treatment significantly reduced the anxiety levels following repeated social defeat, as evident by the higher time spent in central area of open field test, and more time spent in the dark chamber of the light-dark test. Disulfiram and necrosulfonamide treatment also improved working memory in stressed rats, as observed by higher number of entries in the novel arm of Y-maze test **(H)**. All data are presented as mean with 95% CI (n=10-12); p values are indicated for specific pairwise comparisons.

Figure 5. Concurrent inhibition of canonical and non-canonical inflammasomes potentiates anxiolytic effect. **(A)** Canonical pathway was inhibited by MCC950, a specific NLRP3 inhibitor, or ibrutinib, a specific BTK inhibitor. Non-canonical pathway was inhibited by wedelolactone, a caspase 11 inhibitor, or disulfiram, a gasdermin D inhibitor. As compared to individual treatments, a combination treatment with MCC950 and wedelolactone significantly reduced the IL1β levels in

hippocampus **(B)**, and improved working memory in Y-maze test **(C)** in female rats subjected to repeated social defeat. We performed social interaction tests to analyze sociability and social preference **(D)**. Sociability scores were measured by preference of test rat to interact with another rat (rat 1) as compared to empty chamber. Thereafter, social preference was scored by analyzing the preference of test rat to novel rat (rat 2) as compared to familiar rat (rat 1). Combinational treatment to inhibit both canonical and non-canonical inflammasomes by simultaneous treatment with disulfiram and ibrutinib was much more effective to significantly improve sociability **(E)** and social preference indexes **(F)**, as compared to individual treatment of stressed rats. Repeated social defeat-indued anxious behavior is associated with downregulation of dendritic spine density and reduction of mushroom-shaped mature spines. Golgi-cox staining **(G)** was performed to analyze dendritic spine density **(H)** and number of mushroom-shaped spines **(I)** in CA3 region of hippocampus. A combination treatment with disulfiram and ibrutinib significantly inhibited the reduction of spine density and the number of mushroom-shaped mature spines following repeated social defeat in female rats. Similarly, the combination treatment with disulfiram and ibrutinib significantly reduced the neuroinflammation, as evident by significant reduction of mRNA levels of monocyte/macrophage receptor *CCR2* **(J)** and microglial ligand *CCL2* **(K)** in hippocampus of female rats subjected to psychosocial stress. All data are presented as mean with 95% CI (n=10-12); p values are indicated for specific pairwise comparisons.

Figure 6. Combination treatment with disulfiram and ibrutinib synergistically improves anxiolytic effect and working memory. (A) A combination treatment with disulfiram and ibrutinib was carried out from the first stress induction day to total 7 consecutive days. IL1β levels with ELISA and caspase 1 activity were measured in hippocampus and amygdala homogenates of SD rats. The combination treatment significantly reduced the IL1β levels **(B)** and caspase 1 activity **(C)** in the brains of male and female rats subjected to repeated social defeat-induced psychosocial stress. This combination treatment also significantly improved anxiogenic fear memory responses, as evident by reduction of fear acquisition, extinction and recall responses in male **(D)** and female **(E)** stressed rats. To investigate the effects of combination treatment on anxiety-like behavior, light-dark test **(F)** and

open field test **(G)** were performed. Combination treatment significantly reduced the anxiety-like behavior, suggesting strong anxiolytic potential of the combination treatment. Heat map of the novel object recognition task indicated that stressed rats spent lower time with novel object as compared to control rats, as depicted by lesser blue/red color at the top right corner **(H)**. This combination treatment significantly improved working memory function in stressed rats, as evident by the higher time spent with the novel object in the novel object test **(I,J)** and more entries to novel arm of the Y-maze **(J)**. All data are presented as mean with 95% CI (n=10-12); p values are indicated for specific pairwise comparisons.

Figure 7. Psychosocial stress induces caspase 11 and gasdermin D, non-canonical inflammasomes, in PBMCs. (A) Immunoblotting was performed to measure the levels of gasdermin D-N terminal and cleaved caspase 11 from isolated PBMCs of rats with (+) or without (-) psychosocial stress. Densitometric analysis showed significantly higher levels of gasdermin D-N terminal **(B)** and cleaved caspase 11 **(C)** following repeated social defeat. This suggests activation of non-canonical inflammasome pathway in the peripheral immune cells under psychosocial stress. IL1β levels in the culture media of PBMCs from stressed rats were significantly higher as compared to controls, and wedelolactone treatment significantly reduced LPS-induced IL1β levels **(D)**. A combination treatment of MCC950 and wedelolactone was able to significantly reduce the LPS induced IL1β levels **(F)** as it inhibits both NLRP3 and caspase 11. Similarly, concurrent Inhibition of BTK and gasdermin D by ibrutinib and disulfiram combination treatment significantly reduced IL1β levels in LPS induced PBMCs **(G)**. IL1β processing enzyme caspase 1 activity was also significantly reduced with ibrutinib and disulfiram treatment **(H)**. To analyze the pyroptosis – the membrane pore formation by gasdermin D, SYTOX green uptake assay was performed. Higher pore formation causes higher levels of SYTOX green influx into the PBMCs. The treatment with wedelolactone significantly decreased SYTOX green uptake in the PBMCs exposed to LPS **(E)**. As compared to individual treatment, the combination treatment of disulfiram and ibrutinib was more effective in attenuating SYTOX green uptake **(I)**. This suggests caspase 11 and gasdermin D were responsible for membrane

pore formation. Suggestive schematic diagram of canonical and non-canonical NLRP3 inflammasome pathway in psychosocial stress **(J)**. Artwork adapted from https://smart.servier.com, CC BY 4.0. All data are presented as mean with 95% CI (n=10-12); *p<0.05; one-way ANOVA with Bonferroni post hoc test.

Supplementary Figure 1. Physical and psychosocial stress induce corticosterone, caspase 1 and gasdermin D. To evaluate the stress responses under physical **(A)** and psychosocial **(B)** stress in male and female rats, plasma corticosterone level was measured by ELISA assay. Plasma corticosterone levels was significantly increased in females as compared to their male counterparts following physical and psychosocial stress. Immunoblot analysis in from Figure 1 indicated induction of cleaved caspase 1 following psychosocial stress **(C).** To determine the correlation of gasdermin D levels in CSF with time spent by rats in central area of open field test, Pearson correlation analysis for rats with physical stress **(D)** and psychosocial stress **(E)** was performed. Rats subjected to physical and psychosocial stress showed moderate to high negative corelation of gasdermin D levels with time spent in open field test. Caspase 1 activity **(F)** was significantly higher in hippocampus and amygdala of female physically stressed rats as compared to their male counterparts. All data are presented as mean with 95% CI (n=10-12); p values are indicated for specific pairwise comparisons.

Supplementary Figure 2. Wedelolactone treatment attenuates induction of stressed-induced IL1β, caspase 1 and gasdermin D. (A) Wedelolactone treatment significantly reduced IL1β levels in amygdala homogenates of stressed rats. Similarly, wedelolactone treatment also significantly reduced caspase 1 activity in amygdala of stressed rats **(B)**. This treatment also significantly reduced gasdermin D levels in CSF from rats with psychosocial stress **(C)**. Wedelolactone treatment significantly improved working memory, as indicated by increased exploration of novel object in novel object recognition test **(D)**. All data are presented as mean with 95% CI (n=10-12); p values are indicated for specific pairwise comparisons.

Supplementary Figure 3. Psychological stress induces macrophage ligand CXCL2 and endothelial cells adhesion molecule ICAM-1 in brain. The levels of macrophage ligand CXCL2 **(A)** and brain endothelial cells adhesion molecule ICAM-1 **(B)** was measured by ELISA in hippocampal homogenates. Female rats subjected to psychosocial stress showed significantly higher levels of CXCL2 and ICAM-1 in hippocampus than their male counterparts. As compared to individual treatments, the combination treatment with disulfiram and ibrutinib significantly reduced the CXCL2 and ICAM-1 expressions. All data are presented as mean with 95% CI (n=10-12); p values are indicated for specific pairwise comparisons.

Supplementary Figure 4. Combination treatment with disulfiram and ibrutinib attenuates IL1β levels in stressed rats. IL1β levels in plasma **(A)** and CSF **(B)** was measured by ELISA. The combination treatment with disulfiram and ibrutinib significantly reduced IL1β levels in plasma and CSF of rats subjected to psychosocial stress. All data are presented as mean with 95% CI (n=10-12); p values are indicated for specific pairwise comparisons.

Supplementary Figure 5. Inhibition of mediators of inflammasomes suppresses IL1β and caspase 1 in PBMCs from stressed rats. PBMCs were isolated from control and stressed rats and then subjected to various treatments under *in vitro* conditions. Cell viability was measured by WST-8 assay at 3 h following treatment with LPS with or without wedelolactone. **(A)**. There were no significant differences in cell viability between various groups of PBMCs. LPS-induced PBMC from psychosocially stressed female rats showed significantly higher caspase 1 activity **(B)**. Combination treatment with MCC950 and wedelolactone significantly reduced the LPS-induced caspase 1 activity. IL1β levels in PBMC culture media was measured by ELISA. IL1β levels in PBMC culture media was significantly higher in psychosocial stress than the control group **(C)**. Combination treatment with disulfiram and ibrutinib significantly reduced the IL1β levels in PBMCs. Cell viability was measured by WST-8 assay at 3 h following treatment with LPS with or without ibrutinib and disulfiram **(D)**. There were no significant differences in cell viability between various groups of PBMCs. All data are presented as mean with 95% CI (n=10-12); p values are indicated for specific pairwise comparisons.

References

1. GBD 2019 Mental Disorders Collaborators. Global, regional, and national burden of 12 mental disorders in 204 countries and territories, 1990-2019: a systematic analysis for the Global Burden of Disease Study 2019. Lancet Psychiatry. 2022 Feb;9(2):137–50.

2. Arias D, Saxena S, Verguet S. Quantifying the global burden of mental disorders and their economic value. eClinicalMedicine [Internet]. 2022 Dec 1 [cited 2024 Nov 15];54. Available from: https://www.thelancet.com/journals/eclinm/article/PIIS2589-5370(22)00405-9/fulltext

3. Our World in Data [Internet]. [cited 2024 Dec 4]. Number with a mental or neurodevelopmental disorder by type. Available from: https://ourworldindata.org/grapher/number-with-mental-and-neurodevelopmental-disorders-by-type

4. Ojagbemi A, Gureje O. Mental health in low- and middle-income countries. In: Bhugra D, Moussaoui D, Craig TJ, Bhugra D, Moussaoui D, Craig TJ, editors. Oxford Textbook of Social Psychiatry [Internet]. Oxford University Press; 2022 [cited 2024 Feb 6]. p. 0. Available from: https://doi.org/10.1093/med/9780198861478.003.0072

5. Solmi M, Radua J, Olivola M, Croce E, Soardo L, Salazar de Pablo G, et al. Age at onset of mental disorders worldwide: large-scale meta-analysis of 192 epidemiological studies. Mol Psychiatry. 2022 Jan;27(1):281–95.

6. Gururaj G, Gautham MS, Varghese M, Benegal V, Rao GN, Kokane A, et al. The National Mental Health Survey of India (2016): Prevalence, socio-demographic correlates and treatment gap of mental morbidity. Int J Soc Psychiatry. 2020 Jun 1;66(4):361–72.

7. Gautham MS, Gururaj G, Varghese M, Benegal V, Rao GN, Kokane A, et al. The National Mental Health Survey of India (2016): Prevalence, socio-demographic correlates and treatment gap of mental morbidity. International Journal of Social Psychiatry [Internet]. 2020 Mar 4 [cited 2024 Dec 4]; Available from: https://journals.sagepub.com/doi/10.1177/0020764020907941

8. Woelbert E, White R, Lundell-Smith K, Grant J, Kemmer D. The Inequities of Mental Health Research (IAMHRF) [Internet]. Digital Science; 2020 Dec [cited 2024 Dec 4]. Available from: https://digitalscience.figshare.com/articles/report/The_Inequities_of_Mental_Health_Research_IAMHRF_/13055897/2

9. Cipriani A, Furukawa TA, Salanti G, Chaimani A, Atkinson LZ, Ogawa Y, et al. Comparative efficacy and acceptability of 21 antidepressant drugs for the acute treatment of adults with major depressive disorder: a systematic review and network meta-analysis. Lancet. 2018 Apr 7;391(10128):1357–66.

10. Hengartner MP, Jakobsen JC, Sørensen A, Plöderl M. Efficacy of new-generation antidepressants assessed with the Montgomery-Asberg Depression Rating Scale, the gold standard clinician rating scale: A meta-analysis of randomised placebo-controlled trials. PLOS ONE. 2020 Feb 26;15(2):e0229381.

11. Volkmann C, Volkmann A, Müller CA. On the treatment effect heterogeneity of antidepressants in major depression: A Bayesian meta-analysis and simulation study. PLOS ONE. 2020 Nov 11;15(11):e0241497.

12. Guo X, McCutcheon RA, Pillinger T, Mizuno Y, Natesan S, Brown K, et al. The magnitude and heterogeneity of antidepressant response in depression: A meta-analysis of over 45,000 patients. Journal of Affective Disorders. 2020 Nov 1;276:991–1000.

13. He H, Xiang Y, Gao F, Bai L, Gao F, Fan Y, et al. Comparative efficacy and acceptability of first-line drugs for the acute treatment of generalized anxiety disorder in adults: A network meta-analysis. J Psychiatr Res. 2019 Nov;118:21–30.

14. Kong W, Deng H, Wan J, Zhou Y, Zhou Y, Song B, et al. Comparative Remission Rates and Tolerability of Drugs for Generalised Anxiety Disorder: A Systematic Review and Network Meta-analysis of Double-Blind Randomized Controlled Trials. Front Pharmacol. 2020;11:580858.

15. Kim HK, Blumberger DM, Fitzgerald PB, Mulsant BH, Daskalakis ZJ. Antidepressant treatment outcomes in patients with and without comorbid physical or psychiatric disorders: A systematic review and meta-analysis. Journal of Affective Disorders. 2021 Dec 1;295:225–34.

16. COVID-19 Mental Disorders Collaborators. Global prevalence and burden of depressive and anxiety disorders in 204 countries and territories in 2020 due to the COVID-19 pandemic. Lancet. 2021 Nov 6;398(10312):1700–12.

17. Bandelow B, Sher L, Bunevicius R, Hollander E, Kasper S, Zohar J, et al. Guidelines for the pharmacological treatment of anxiety disorders, obsessive–compulsive disorder and posttraumatic stress disorder in primary care. International Journal of Psychiatry in Clinical Practice. 2012 Jun 1;16(2):77–84.

18. Baldwin DS, Anderson IM, Nutt DJ, Allgulander C, Bandelow B, den Boer JA, et al. Evidence-based pharmacological treatment of anxiety disorders, post-traumatic stress disorder and obsessive-compulsive disorder: A revision of the 2005 guidelines from the British Association for Psychopharmacology. J Psychopharmacol. 2014 May 1;28(5):403–39.

19. Hoskins M, Pearce J, Bethell A, Dankova L, Barbui C, Tol WA, et al. Pharmacotherapy for post-traumatic stress disorder: Systematic review and meta-analysis. The British Journal of Psychiatry. 2015 Feb;206(2):93–100.

20. Jakubovski E, Varigonda AL, Freemantle N, Taylor MJ, Bloch MH. Systematic Review and Meta-Analysis: Dose-Response Relationship of Selective Serotonin Reuptake Inhibitors in Major Depressive Disorder. AJP. 2016 Feb;173(2):174–83.

21. Szuhany KL, Simon NM. Anxiety Disorders: A Review. JAMA. 2022 Dec 27;328(24):2431–45.

22. Gunnell D, Saperia J, Ashby D. Selective serotonin reuptake inhibitors (SSRIs) and suicide in adults: meta-analysis of drug company data from placebo controlled, randomised controlled trials submitted to the MHRA's safety review. BMJ. 2005 Feb 17;330(7488):385.

23. Gibbons RD, Brown CH, Hur K, Marcus SM, Bhaumik DK, Erkens JA, et al. Early Evidence on the Effects of Regulators' Suicidality Warnings on SSRI Prescriptions and Suicide in Children and Adolescents. AJP. 2007 Sep;164(9):1356–63.

24. Strawn JR, Mills JA, Poweleit EA, Ramsey LB, Croarkin PE. Adverse Effects of Antidepressant Medications and their Management in Children and Adolescents. Pharmacotherapy: The Journal of Human Pharmacology and Drug Therapy. 2023;43(7):675–90.

25. Vogelzangs N, Beekman ATF, de Jonge P, Penninx BWJH. Anxiety disorders and inflammation in a large adult cohort. Transl Psychiatry. 2013 Apr;3(4):e249–e249.

26. Gaspersz R, Lamers F, Wittenberg G, Beekman ATF, van Hemert AM, Schoevers RA, et al. The role of anxious distress in immune dysregulation in patients with major depressive disorder. Transl Psychiatry. 2017 Dec 8;7(12):1–12.

27. Morrison FG, Miller MW, Wolf EJ, Logue MW, Maniates H, Kwasnik D, et al. Reduced interleukin 1A gene expression in the dorsolateral prefrontal cortex of individuals with PTSD and depression. Neuroscience Letters. 2019 Jan 23;692:204–9.

28. Milaneschi Y, Kappelmann N, Ye Z, Lamers F, Moser S, Jones PB, et al. Association of inflammation with depression and anxiety: evidence for symptom-specificity and potential causality from UK Biobank and NESDA cohorts. Mol Psychiatry. 2021 Dec;26(12):7393–402.

29. Vogelzangs N, de Jonge P, Smit JH, Bahn S, Penninx BW. Cytokine production capacity in depression and anxiety. Transl Psychiatry. 2016 May;6(5):e825–e825.

30. Heneka MT, Kummer MP, Latz E. Innate immune activation in neurodegenerative disease. Nature Publishing Group; 2014.

31. Heneka MT, O'Banion MK. Inflammatory processes in Alzheimer's disease. 2007.

32. Pawluk H, Woźniak A, Grześk G, Kołodziejska R, Kozakiewicz M, Kopkowska E, et al. The Role of Selected Pro-Inflammatory Cytokines in Pathogenesis of Ischemic Stroke. Clinical Interventions in Aging [Internet]. 2020 Mar 23 [cited 2025 Feb 1]; Available from: https://www.tandfonline.com/doi/abs/10.2147/CIA.S233909

33. Bodnar CN, Watson JB, Higgins EK, Quan N, Bachstetter AD. Inflammatory Regulation of CNS Barriers After Traumatic Brain Injury: A Tale Directed by Interleukin-1. Front Immunol [Internet]. 2021 May 21 [cited 2025 Feb 1];12. Available from: https://www.frontiersin.org/journals/immunology/articles/10.3389/fimmu.2021.688254/full

34. Malik S, Alnaji O, Malik M, Gambale T, Farrokhyar F, Rathbone MP. Inflammatory cytokines associated with mild traumatic brain injury and clinical outcomes: a systematic review and meta-analysis. Front Neurol [Internet]. 2023 May 12 [cited 2025 Feb 1];14.

Available from:
https://www.frontiersin.org/journals/neurology/articles/10.3389/fneur.2023.1123407/full

35. Granowitz E, Clark B, Vannier E, Callahan M, Dinarello C. Effect of interleukin-1 (IL-1) blockade on cytokine synthesis: I. IL-1 receptor antagonist inhibits IL-1-induced cytokine synthesis and blocks the binding of IL-1 to its type II receptor on human monocytes. Blood. 1992 May 1;79(9):2356–63.

36. Jura J, Węgrzyn P, Korostyński M, Guzik K, Oczko-Wojciechowska M, Jarząb M, et al. Identification of interleukin-1 and interleukin-6-responsive genes in human monocyte-derived macrophages using microarrays. Biochimica et Biophysica Acta (BBA) - Gene Regulatory Mechanisms. 2008 Jun 1;1779(6):383–9.

37. Weber A, Wasiliew P, Kracht M. Interleukin-1 (IL-1) Pathway. Science Signaling. 2010 Jan 19;3(105):cm1–cm1.

38. Huang Y, Xu W, Zhou R. NLRP3 inflammasome activation and cell death. Cell Mol Immunol. 2021 Sep;18(9):2114–27.

39. Swanson KV, Deng M, Ting JPY. The NLRP3 inflammasome: molecular activation and regulation to therapeutics. Nat Rev Immunol. 2019 Aug;19(8):477–89.

40. Makoni NJ, Nichols MR. The intricate biophysical puzzle of caspase-1 activation. Archives of Biochemistry and Biophysics. 2021 Mar 15;699:108753.

41. Song L, Pei L, Yao S, Wu Y, Shang Y. NLRP3 inflammasome in neurological diseases, from functions to therapies. Frontiers Media S.A.; 2017.

42. Dong Y, Li S, Lu Y, Li X, Liao Y, Peng Z, et al. Stress-induced NLRP3 inflammasome activation negatively regulates fear memory in mice. Journal of Neuroinflammation. 2020 Jul 7;17(1).

43. Pandey GN, Zhang H, Sharma A, Ren X. Innate immunity receptors in depression and suicide: upregulated NOD-like receptors containing pyrin (NLRPs) and hyperactive inflammasomes in the postmortem brains of people who were depressed and died by suicide. Journal of Psychiatry and Neuroscience. 2021 Sep 29;46(5):E538–47.

44. Alcocer-Gómez E, Miguel M de, Casas-Barquero N, Núñez-Vasco J, Sánchez-Alcazar JA, Fernández-Rodríguez A, et al. NLRP3 inflammasome is activated in mononuclear blood cells from patients with major depressive disorder. Brain, Behavior, and Immunity. 2014 Feb;36:111–7.

45. Zhang Y, Liu L, Liu YZ, Shen XL, Wu TY, Zhang T, et al. NLRP3 inflammasome mediates chronic mild stress-induced depression in mice via neuroinflammation. International Journal of Neuropsychopharmacology. 2015 Jun;18(8):1–8.

46. Alcocer-Gómez E, Ulecia-Morón C, Marín-Aguilar F, Rybkina T, Casas-Barquero N, Ruiz-Cabello J, et al. Stress-Induced Depressive Behaviors Require a Functional NLRP3 Inflammasome. Molecular Neurobiology. 2016 Sep;53(7):4874–82.

47. Wong ML, Inserra A, Lewis MD, Mastronardi CA, Leong L, Choo J, et al. Inflammasome signaling affects anxiety- and depressive-like behavior and gut microbiome composition. Mol Psychiatry. 2016 Jun;21(6):797–805.

48. Ghosh S, Mohammed Z, Singh I. Bruton's tyrosine kinase drives neuroinflammation and anxiogenic behavior in mouse models of stress. J Neuroinflammation. 2021 Dec 11;18(1):289.

49. Burdette BE, Esparza AN, Zhu H, Wang S. Gasdermin D in pyroptosis. Acta Pharmaceutica Sinica B. 2021 Sep 1;11(9):2768–82.

50. Kayagaki N, Stowe IB, Lee BL, O'Rourke K, Anderson K, Warming S, et al. Caspase-11 cleaves gasdermin D for non-canonical inflammasome signalling. Nature. 2015 Oct;526(7575):666–71.

51. Shi J, Zhao Y, Wang K, Shi X, Wang Y, Huang H, et al. Cleavage of GSDMD by inflammatory caspases determines pyroptotic cell death. Nature. 2015 Oct 29;526(7575):660–5.

52. Ding J, Wang K, Liu W, She Y, Sun Q, Shi J, et al. Pore-forming activity and structural autoinhibition of the gasdermin family. Nature. 2016 Jul 7;535(7610):111–6.

53. Liu X, Zhang Z, Ruan J, Pan Y, Magupalli VG, Wu H, et al. Inflammasome-activated gasdermin D causes pyroptosis by forming membrane pores. Nature. 2016 Jul;535(7610):153–8.

54. Evavold CL, Ruan J, Tan Y, Xia S, Wu H, Kagan JC. The Pore-Forming Protein Gasdermin D Regulates Interleukin-1 Secretion from Living Macrophages. Immunity. 2018 Jan 16;48(1):35-44.e6.

55. Gao J, Qiu X, Xi G, Liu H, Zhang F, Lv T, et al. Downregulation of GSDMD attenuates tumor proliferation via the intrinsic mitochondrial apoptotic pathway and inhibition of EGFR/Akt signaling and predicts a good prognosis in non-small cell lung cancer. Oncology Reports. 2018 Oct 1;40(4):1971–84.

56. Peng J, Jiang H, Guo J, Huang J, Yuan Q, Xie J, et al. CD147 Expression Is Associated with Tumor Proliferation in Bladder Cancer via GSDMD. BioMed Research International. 2020;2020(1):7638975.

57. Qiu S, Hu Y, Dong S. Pan-cancer analysis reveals the expression, genetic alteration and prognosis of pyroptosis key gene *GSDMD*. International Immunopharmacology. 2021 Dec 1;101:108270.

58. Kayagaki N, Warming S, Lamkanfi M, Walle LV, Louie S, Dong J, et al. Non-canonical inflammasome activation targets caspase-11. Nature. 2011 Nov;479(7371):117–21.

59. Cheng KT, Xiong S, Ye Z, Hong Z, Di A, Tsang KM, et al. Caspase-11–mediated endothelial pyroptosis underlies endotoxemia-induced lung injury. J Clin Invest. 2017 Nov 1;127(11):4124–35.

60. Kenealy S, Manils J, Raverdeau M, Munoz-Wolf N, Barber G, Liddicoat A, et al. Caspase-11–Mediated Cell Death Contributes to the Pathogenesis of Imiquimod-Induced Psoriasis. J Invest Dermatol. 2019 Nov 1;139(11):2389-2393.e3.

61. Lu Y, Meng R, Wang X, Xu Y, Tang Y, Wu J, et al. Caspase-11 signaling enhances graft-versus-host disease. Nat Commun. 2019 Sep 6;10(1):4044.

62. Zasłona Z, Flis E, Wilk MM, Carroll RG, Palsson-McDermott EM, Hughes MM, et al. Caspase-11 promotes allergic airway inflammation. Nat Commun. 2020 Feb 26;11(1):1055.

63. Li S, Sun Y, Song M, Song Y, Fang Y, Zhang Q, et al. NLRP3/caspase-1/GSDMD–mediated pyroptosis exerts a crucial role in astrocyte pathological injury in mouse model of depression. JCI Insight [Internet]. 2021 Dec 8 [cited 2024 Nov 16];6(23). Available from: https://insight.jci.org/articles/view/146852

64. Wang B, Chen SM, Yang SQ, Jiang JM, Zhang P, Zou W, et al. GDF11 mediates H2S to prevent chronic stress-induced cognitive impairment by reducing hippocampal NLRP3/caspase-1-dependent pyroptosis. Journal of Affective Disorders. 2024 Jan 1;344:600–11.

65. Gao H, Li W, Xu S, Xu Z, Hu W, Pan L, et al. Gasdermin D promotes development of intestinal tumors through regulating IL-1β release and gut microbiota composition. Cell Commun Signal. 2024 Oct 21;22(1):511.

66. Hammels C, Pishva E, De Vry J, van den Hove DLA, Prickaerts J, van Winkel R, et al. Defeat stress in rodents: From behavior to molecules. Neuroscience & Biobehavioral Reviews. 2015 Dec 1;59:111–40.

67. Kranzler HR, Soyka M. Diagnosis and Pharmacotherapy of Alcohol Use Disorder: A Review. JAMA. 2018 Aug 28;320(8):815–24.

68. Hu JJ, Liu X, Xia S, Zhang Z, Zhang Y, Zhao J, et al. FDA-approved disulfiram inhibits pyroptosis by blocking gasdermin D pore formation. Nat Immunol. 2020 Jul;21(7):736–45.

69. Zhuang L, Luo X, Wu S, Lin Z, Zhang Y, Zhai Z, et al. Disulfiram alleviates pristane-induced lupus via inhibiting GSDMD-mediated pyroptosis. Cell Death Discov. 2022 Sep 3;8(1):1–9.

70. Kapoor P, Ansell SM. Acalabrutinib in mantle cell lymphoma. The Lancet. 2018;391(10121):633–4.

71. Claro RA, McGinn KM, Verdun N, Lee SL, Chiu HJ, Saber H, et al. FDA approval: Ibrutinib for patients with previously treated mantle cell lymphoma and previously treated chronic lymphocytic leukemia. Clinical Cancer Research. 2015;21(16):3586–90.

72. Wu Y, Pan B, Zhang Z, Li X, Leng Y, Ji Y, et al. Caspase-4/11–Mediated Pulmonary Artery Endothelial Cell Pyroptosis Contributes to Pulmonary Arterial Hypertension. Hypertension. 2022 Mar;79(3):536–48.

73. Rathkey JK, Zhao J, Liu Z, Chen Y, Yang J, Kondolf HC, et al. Chemical disruption of the pyroptotic pore-forming protein gasdermin D inhibits inflammatory cell death and sepsis. Science Immunology. 2018 Aug 24;3(26):eaat2738.

74. Kobori M, Yang Z, Gong D, Heissmeyer V, Zhu H, Jung YK, et al. Wedelolactone suppresses LPS-induced caspase-11 expression by directly inhibiting the IKK Complex. Cell Death Differ. 2004 Jan;11(1):123–30.

75. Miczek KA, de Boer SF, Haller J. Excessive aggression as model of violence: a critical evaluation of current preclinical methods. Psychopharmacology. 2013 Apr 1;226(3):445–58.

76. Prut L, Belzung C. The open field as a paradigm to measure the effects of drugs on anxiety-like behaviors: A review. European Journal of Pharmacology. 2003.

77. Carola V, D'Olimpio F, Brunamonti E, Mangia F, Renzi P. Evaluation of the elevated plus-maze and open-field tests for the assessment of anxiety-related behaviour in inbred mice. Behavioural Brain Research. 2002;

78. Arrant AE, Schramm-Sapyta NL, Kuhn CM. Use of the light/dark test for anxiety in adult and adolescent male rats. Behavioural Brain Research. 2013 Nov 1;256:119–27.

79. Koert A, Ploeger A, Bockting CLH, Schmidt MV, Lucassen PJ, Schrantee A, et al. The social instability stress paradigm in rat and mouse: A systematic review of protocols, limitations, and recommendations. Neurobiology of Stress. 2021 Nov 1;15:100410.

80. Leger M, Quiedeville A, Bouet V, Haelewyn B, Boulouard M, Schumann-Bard P, et al. Object recognition test in mice. Nat Protoc. 2013 Dec;8(12):2531–7.

81. Conrad CD, Lupien SJ, Thanasoulis LC, McEwen BS. The effects of Type I and Type II corticosteroid receptor agonists on exploratory behavior and spatial memory in the Y-maze. Brain Research. 1997 Jun 6;759(1):76–83.

82. Dagnino-Subiabre A, Pérez MÁ, Terreros G, Cheng MY, House P, Sapolsky R. Corticosterone treatment impairs auditory fear learning and the dendritic morphology of the rat inferior colliculus. Hearing Research. 2012 Dec 1;294(1):104–13.

83. Thrivikraman KV, Huot RL, Plotsky PM. Jugular vein catheterization for repeated blood sampling in the unrestrained conscious rat. Brain Research Protocols. 2002 Oct 1;10(2):84–94.

84. Das G, Reuhl K, Zhou R. The Golgi–Cox Method. In: Zhou R, Mei L, editors. Neural Development: Methods and Protocols [Internet]. Totowa, NJ: Humana Press; 2013 [cited 2025 Feb 1]. p. 313–21. Available from: https://doi.org/10.1007/978-1-62703-444-9_29

85. Zhong F, Liu L, Wei JL, Dai RP. Step by Step Golgi-Cox Staining for Cryosection. Front Neuroanat [Internet]. 2019 Jun 19 [cited 2025 Jan 27];13. Available from: https://www.frontiersin.org/journals/neuroanatomy/articles/10.3389/fnana.2019.00062/full

86. Patel D, Anilkumar S, Chattarji S, Buwalda B. Repeated social stress leads to contrasting patterns of structural plasticity in the amygdala and hippocampus. Behavioural Brain Research. 2018 Jul 16;347:314–24.

87. Tominaga H, Ishiyama M, Ohseto F, Sasamoto K, Hamamoto T, Suzuki K, et al. A water-soluble tetrazolium salt useful for colorimetric cell viability assay. Anal Commun. 1999 Jan 1;36(2):47–50.

88. Chauhan D, Demon D, Vande Walle L, Paerewijck O, Zecchin A, Bosseler L, et al. GSDMD drives canonical inflammasome-induced neutrophil pyroptosis and is dispensable for NETosis. EMBO reports. 2022 Oct 6;23(10):e54277.

89. Mehla J, Singh I, Diwan D, Nelson JW, Lawrence M, Lee E, et al. STAT3 inhibitor mitigates cerebral amyloid angiopathy and parenchymal amyloid plaques while improving cognitive functions and brain networks. acta neuropathol commun. 2021 Dec 15;9(1):193.

90. Livak KJ, Schmittgen TD. Analysis of Relative Gene Expression Data Using Real-Time Quantitative PCR and the 2−ΔΔCT Method. Methods. 2001 Dec 1;25(4):402–8.

91. Runge K, Cardoso C, de Chevigny A. Dendritic Spine Plasticity: Function and Mechanisms. Front Synaptic Neurosci [Internet]. 2020 Aug 28 [cited 2025 Jan 13];12. Available from: https://www.frontiersin.org/journals/synaptic-neuroscience/articles/10.3389/fnsyn.2020.00036/full

92. Helm MS, Dankovich TM, Mandad S, Rammner B, Jähne S, Salimi V, et al. A large-scale nanoscopy and biochemistry analysis of postsynaptic dendritic spines. Nat Neurosci. 2021 Aug;24(8):1151–62.

93. Soetanto A, Wilson RS, Talbot K, Un A, Schneider JA, Sobiesk M, et al. Association of Anxiety and Depression With Microtubule-Associated Protein 2– and Synaptopodin-Immunolabeled Dendrite and Spine Densities in Hippocampal CA3 of Older Humans. Archives of General Psychiatry. 2010 May 1;67(5):448–57.

94. Qiao H, Li MX, Xu C, Chen HB, An SC, Ma XM. Dendritic Spines in Depression: What We Learned from Animal Models. Neural Plasticity. 2016;2016(1):8056370.

95. Qu Y, Yang C, Ren Q, Ma M, Dong C, Hashimoto K. Regional differences in dendritic spine density confer resilience to chronic social defeat stress. Acta Neuropsychiatrica. 2018 Apr;30(2):117–22.

96. Shaftel SS, Carlson TJ, Olschowka JA, Kyrkanides S, Matousek SB, O'Banion MK. Chronic Interleukin-1β Expression in Mouse Brain Leads to Leukocyte Infiltration and Neutrophil-Independent Blood–Brain Barrier Permeability without Overt Neurodegeneration. J Neurosci. 2007 Aug 29;27(35):9301–9.

97. Wohleb ES, Powell ND, Godbout JP, Sheridan JF. Stress-induced recruitment of bone marrow-derived monocytes to the brain promotes anxiety-like behavior. J Neurosci. 2013 Aug 21;33(34):13820–33.

98. Wohleb ES, McKim DB, Sheridan JF, Godbout JP. Monocyte trafficking to the brain with stress and inflammation: a novel axis of immune-to-brain communication that influences mood and behavior. Front Neurosci [Internet]. 2015 Jan 21 [cited 2024 Dec 19];8. Available from: https://www.frontiersin.org/journals/neuroscience/articles/10.3389/fnins.2014.00447/full

99. Sawicki CM, McKim DB, Wohleb ES, Jarrett BL, Reader BF, Norden DM, et al. Social defeat promotes a reactive endothelium in a brain region-dependent manner with increased expression of key adhesion molecules, selectins and chemokines associated with the recruitment of myeloid cells to the brain. Neuroscience. 2015 Aug 27;302:151–64.

100. McKim DB, Weber MD, Niraula A, Sawicki CM, Liu X, Jarrett BL, et al. Microglial recruitment of IL-1β-producing monocytes to brain endothelium causes stress-induced anxiety. Mol Psychiatry. 2018 Jun;23(6):1421–31.

101. Sithu SD, English WR, Olson P, Krubasik D, Baker AH, Murphy G, et al. Membrane-type 1-Matrix Metalloproteinase Regulates Intracellular Adhesion Molecule-1 (ICAM-1)-mediated Monocyte Transmigration *. Journal of Biological Chemistry. 2007 Aug 24;282(34):25010–9.

102. Wohleb ES, Patterson JM, Sharma V, Quan N, Godbout JP, Sheridan JF. Knockdown of Interleukin-1 Receptor Type-1 on Endothelial Cells Attenuated Stress-Induced Neuroinflammation and Prevented Anxiety-Like Behavior. J Neurosci. 2014 Feb 12;34(7):2583–91.

103. Yin W, Swanson SP, Biltz RG, Goodman EJ, Gallagher NR, Sheridan JF, et al. Unique brain endothelial profiles activated by social stress promote cell adhesion, prostaglandin E2 signaling, hypothalamic–pituitary–adrenal axis modulation, and anxiety. Neuropsychopharmacol. 2022 Dec;47(13):2271–82.

104. Boro M, Balaji KN. CXCL1 and CXCL2 Regulate NLRP3 Inflammasome Activation via G-Protein–Coupled Receptor CXCR2. The Journal of Immunology. 2017 Sep 1;199(5):1660–71.

105. Wu F, Zhao Y, Jiao T, Shi D, Zhu X, Zhang M, et al. CXCR2 is essential for cerebral endothelial activation and leukocyte recruitment during neuroinflammation. J Neuroinflammation. 2015 May 21;12(1):98.

106. Ma K, An C, Li M, Zhang Y, Ren M, Wei Y, et al. Dexmedetomidine Attenuated Neuron Death, Cognitive Decline, and Anxiety-Like Behavior by Inhibiting CXCL2 in CA1 Region of AD Mice. Drug Design, Development and Therapy. 2024 Dec 31;18:5351–65.

107. Cerretti DP, Kozlosky CJ, Mosley B, Nelson N, Van Ness K, Greenstreet TA, et al. Molecular Cloning of the Interleukin-1β Converting Enzyme. Science. 1992 Apr 3;256(5053):97–100.

108. Thornberry NA, Bull HG, Calaycay JR, Chapman KT, Howard AD, Kostura MJ, et al. A novel heterodimeric cysteine protease is required for interleukin-1βprocessing in monocytes. Nature. 1992 Apr;356(6372):768–74.

109. Wang S, Miura M, Jung Y keun, Zhu H, Gagliardini V, Shi L, et al. Identification and Characterization of Ich-3, a Member of the Interleukin-1β Converting Enzyme (ICE)/Ced-3 Family and an Upstream Regulator of ICE *. Journal of Biological Chemistry. 1996 Aug 23;271(34):20580–7.

110. Lieberman J, Wu H, Kagan JC. Gasdermin D activity in inflammation and host defense. Science Immunology. 2019 Sep 6;4(39):eaav1447.

111. Claude L, Martino F, Hermand P, Chahim B, Roger P, de Bourayne M, et al. Platelet caspase-1 and Bruton tyrosine kinase activation in patients with COVID-19 is associated with disease severity and reversed in vitro by ibrutinib. Research and Practice in Thrombosis and Haemostasis. 2022 Nov 1;6(8):e12811.

112. Tang H, Li H, Yang Y, Tang M, Li Z, Bai X, et al. Ibrutinib protects against acute lung injury via inhibiting NLRP3/Caspase-1 in septic mice model. Molecular Immunology. 2022 Dec 1;152:232–9.

113. Vogel S, Kamimura S, Smith ML, Nguyen E, Zerfas P, Almeida LEF, et al. NLRP3 Inflammasome-Mediated Platelet Activation and Thrombus Formation in Sickle Cell Mice Can be Targeted By the BTK Inhibitor Ibrutinib. Blood. 2023 Nov 2;142:3935.

114. Krohn TC, Sørensen DB, Ottesen JL, Hansen AK. The effects of individual housing on mice and rats: a review. Animal Welfare. 2006 Nov;15(4):343–52.

115. Levine J, Barak Y, Chengappa KNR, Rapoport A, Rebey M, Barak V. Cerebrospinal Cytokine Levels in Patients with Acute Depression. Neuropsychobiology. 1999 Nov 4;40(4):171–6.

116. Martinez JM, Garakani A, Yehuda R, Gorman JM. Proinflammatory and "Resiliency" Proteins in the Csf of Patients with Major Depression. Depression and Anxiety. 2012;29(1):32–8.

117. Enokida T, Hattori K, Okabe K, Noda T, Ota M, Sato N, et al. Possible association of elevated CSF IL-6 levels with anxiety and frustration in psychiatric disorders. Psychiatry and Clinical Neurosciences [Internet]. 2024 [cited 2024 Nov 20];n/a(n/a). Available from: https://onlinelibrary.wiley.com/doi/abs/10.1111/pcn.13743

118. Hein AM, Zarcone TJ, Parfitt DB, Matousek SB, Carbonari DM, Olschowka JA, et al. Behavioral, structural and molecular changes following long-term hippocampal IL-1β overexpression in transgenic mice. J Neuroimmune Pharmacol. 2012 Mar;7(1):145–55.

119. Hein AM, Stasko MR, Matousek SB, Scott-McKean JJ, Maier SF, Olschowka JA, et al. Sustained hippocampal IL-1beta overexpression impairs contextual and spatial memory in transgenic mice. Brain Behav Immun. 2010 Feb;24(2):243–53.

120. Moore AH, Wu M, Shaftel SS, Graham KA, O'Banion MK. Sustained expression of interleukin-1beta in mouse hippocampus impairs spatial memory. Neuroscience. 2009 Dec 29;164(4):1484–95.

121. Strohm AO, Oldfield S, Hernady E, Johnston CJ, Marples B, O'Banion MK, et al. Biological sex, microglial signaling pathways, and radiation exposure shape cortical proteomic profiles and behavior in mice. Brain Behav Immun Health. 2025 Feb;43:100911.

122. Han J, Fan Y, Zhou K, Blomgren K, Harris RA. Uncovering sex differences of rodent microglia. Journal of Neuroinflammation. 2021 Mar 17;18(1):74.

123. Saitoh A, Nagayama Y, Yamada D, Makino K, Yoshioka T, Yamanaka N, et al. Disulfiram Produces Potent Anxiolytic-Like Effects Without Benzodiazepine Anxiolytics-Related Adverse Effects in Mice. Front Pharmacol [Internet]. 2022 Mar 7 [cited 2024 Dec 20];13. Available from: https://www.frontiersin.org/journals/pharmacology/articles/10.3389/fphar.2022.826783/full

Figure 1

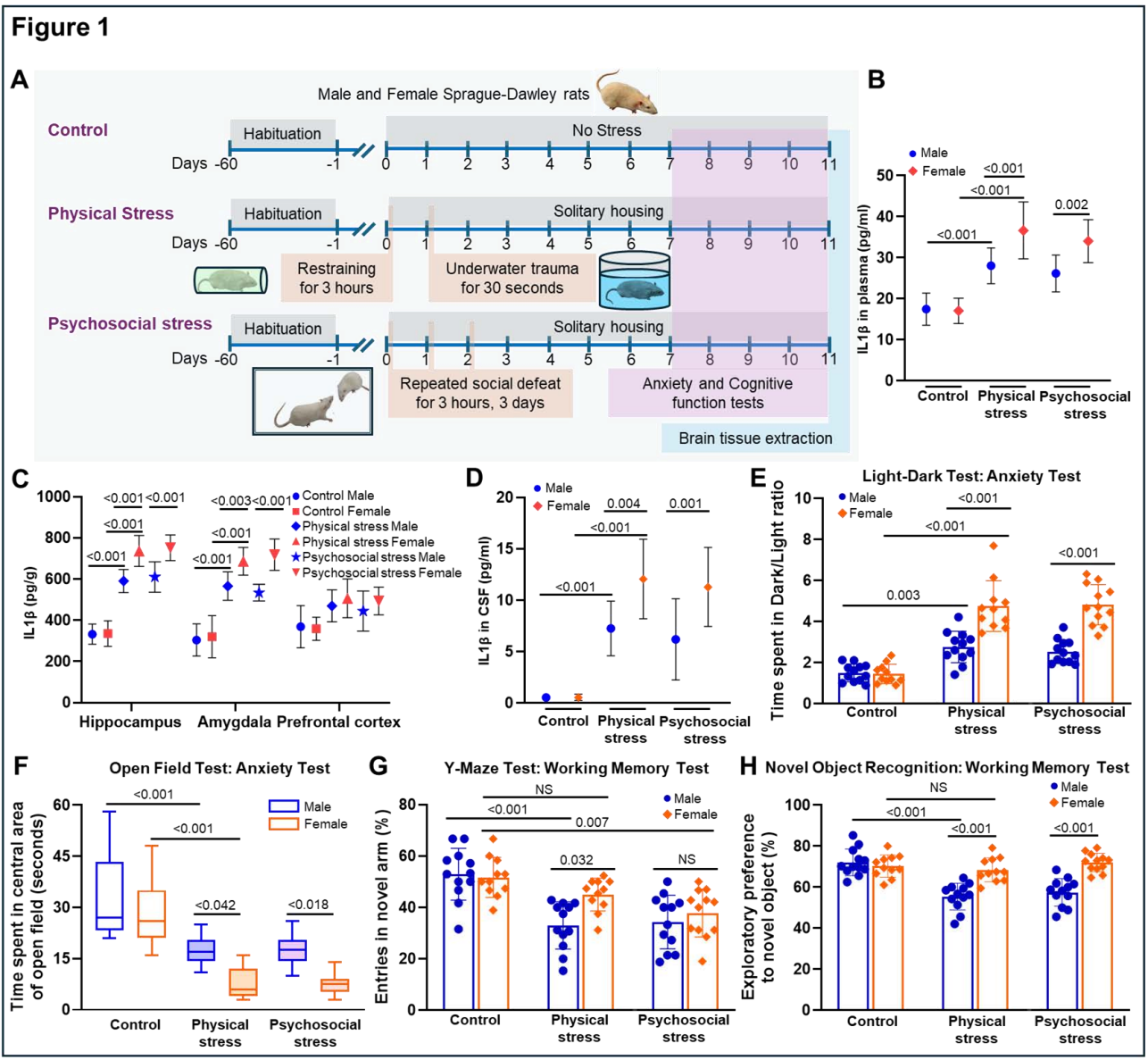
A
Male and Female Sprague-Dawley rats
Control
Habituation
No Stress
Days -60 -1 0 1 2 3 4 5 6 7 8 9 10 11
Physical Stress
Habituation
Solitary housing
Restraining for 3 hours
Underwater trauma for 30 seconds
Psychosocial stress
Habituation
Solitary housing
Repeated social defeat for 3 hours, 3 days
Anxiety and Cognitive function tests
Brain tissue extraction
B
Male
Female
IL1β in plasma (pg/ml)
<0.001
<0.001
<0.001
0.002
Control
Physical stress
Psychosocial stress
C
IL1β (pg/g)
Control Male
Control Female
Physical stress Male
Physical stress Female
Psychosocial stress Male
Psychosocial stress Female
<0.001
<0.001
<0.001
<0.001
<0.003
<0.001
<0.001
<0.001
Hippocampus
Amygdala
Prefrontal cortex
D
Male
Female
IL1β in CSF (pg/ml)
<0.001
<0.001
0.004
0.001
Control
Physical stress
Psychosocial stress
E
Light-Dark Test: Anxiety Test
Male
Female
Time spent in Dark/Light ratio
<0.001
<0.001
0.003
<0.001
Control
Physical stress
Psychosocial stress
F
Open Field Test: Anxiety Test
Male
Female
Time spent in central area of open field (seconds)
<0.001
<0.001
<0.042
<0.018
Control
Physical stress
Psychosocial stress
G
Y-Maze Test: Working Memory Test
Male
Female
Entries in novel arm (%)
NS
<0.001
0.007
0.032
NS
Control
Physical stress
Psychosocial stress
H
Novel Object Recognition: Working Memory Test
Male
Female
Exploratory preference to novel object (%)
NS
<0.001
<0.001
<0.001
Control
Physical stress
Psychosocial stress

Figure 2

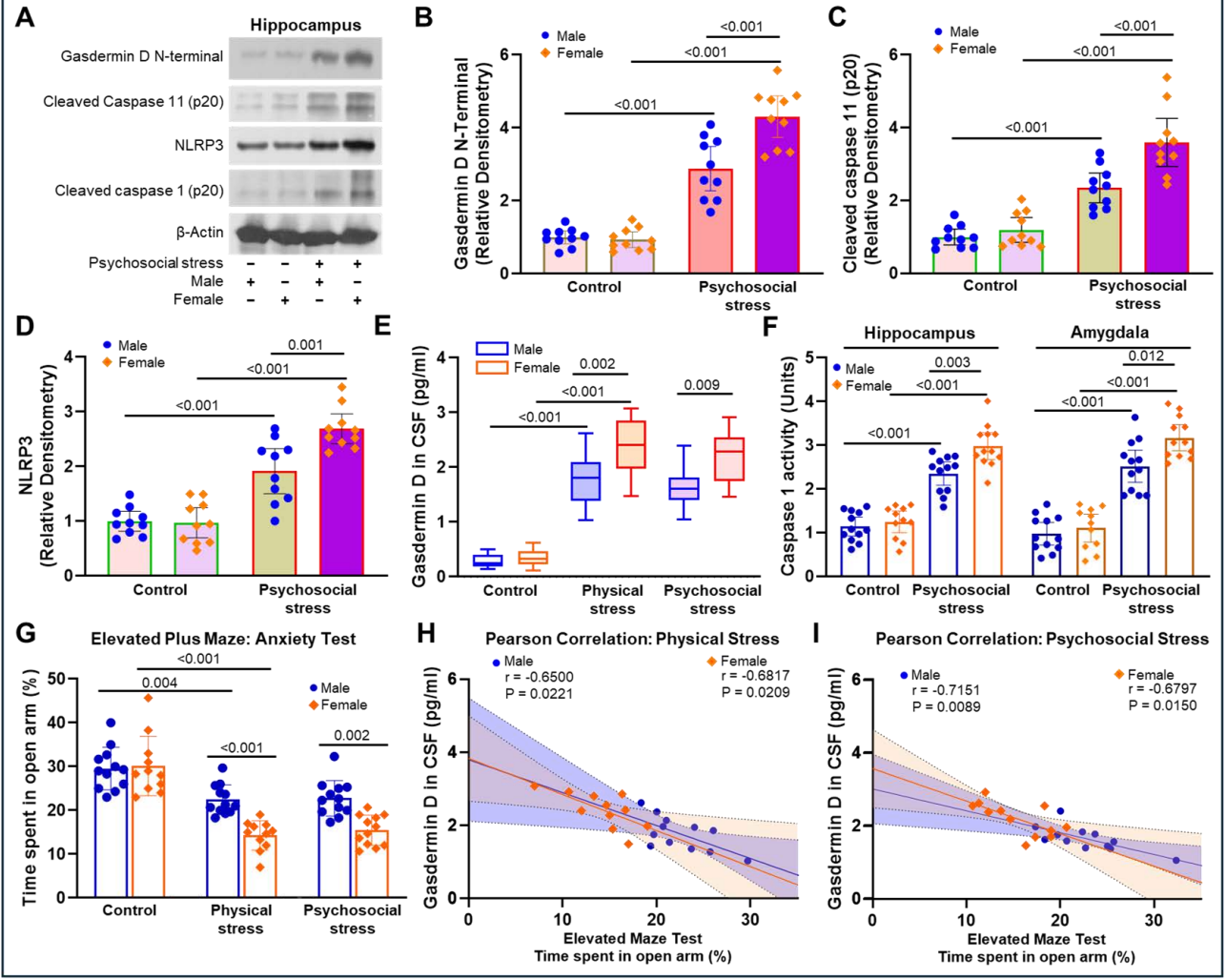
A
Hippocampus
Gasdermin D N-terminal
Cleaved Caspase 11 (p20)
NLRP3
Cleaved caspase 1 (p20)
β-Actin
Psychosocial stress
Male
Female
B
Male
Female
Gasdermin D N-Terminal (Relative Densitometry)
Control
Psychosocial stress
C
Cleaved caspase 11 (p20) (Relative Densitometry)
D
NLRP3 (Relative Densitometry)
E
Gasdermin D in CSF (pg/ml)
Physical stress
F
Hippocampus
Amygdala
Caspase 1 activity (Units)
G
Elevated Plus Maze: Anxiety Test
Time spent in open arm (%)
H
Pearson Correlation: Physical Stress
Male
r = -0.6500
P = 0.0221
Female
r = -0.6817
P = 0.0209
Elevated Maze Test
Time spent in open arm (%)
I
Pearson Correlation: Psychosocial Stress
Male
r = -0.7151
P = 0.0089
Female
r = -0.6797
P = 0.0150

Figure 3

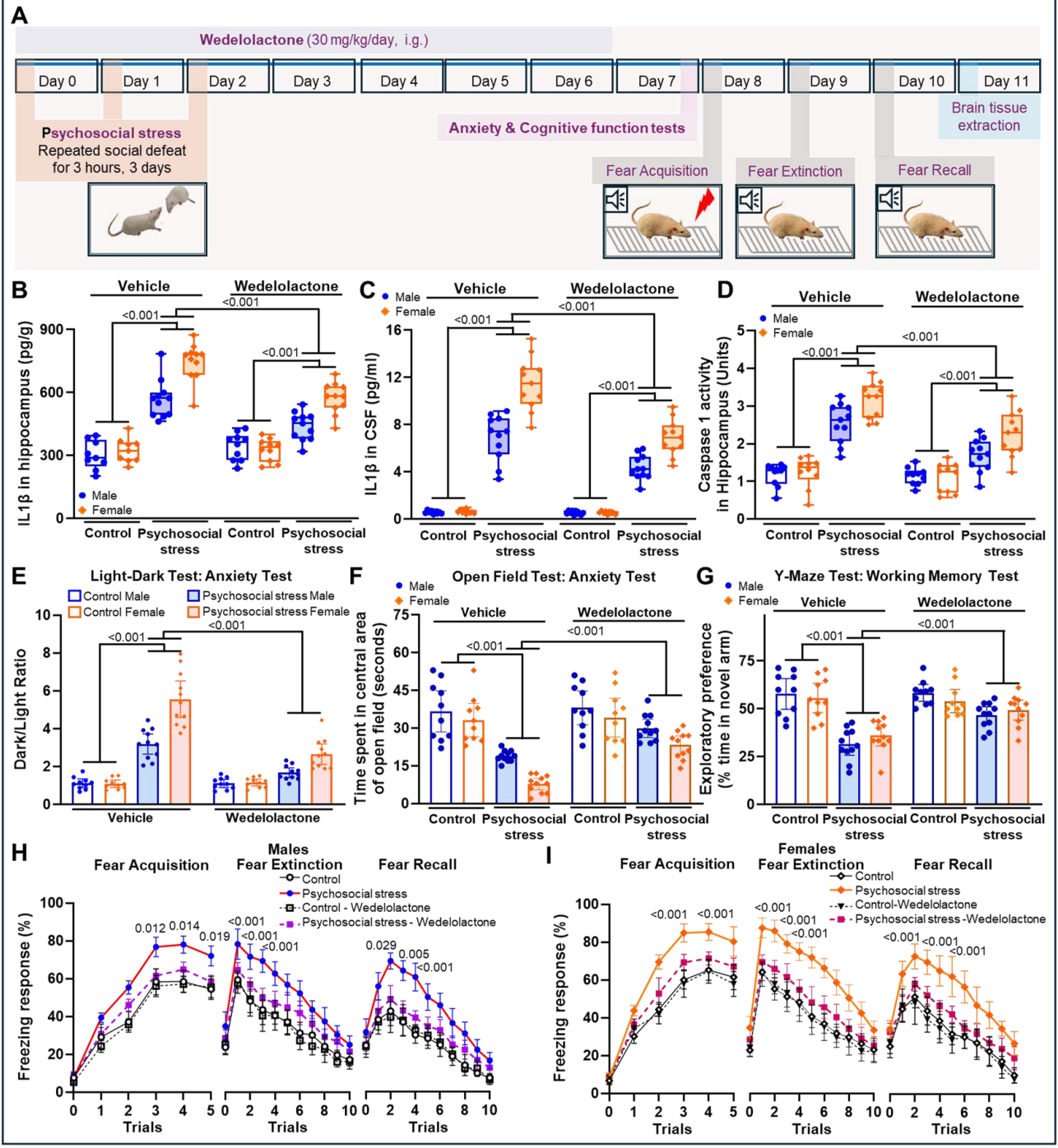
A
Wedelolactone (30 mg/kg/day, i.g.)
Day 0
Day 1
Day 2
Day 3
Day 4
Day 5
Day 6
Day 7
Day 8
Day 9
Day 10
Day 11
Psychosocial stress
Repeated social defeat for 3 hours, 3 days
Anxiety & Cognitive function tests
Brain tissue extraction
Fear Acquisition
Fear Extinction
Fear Recall
B
Vehicle
Wedelolactone
IL1β in hippocampus (pg/g)
Male
Female
Control
Psychosocial stress
C
IL1β in CSF (pg/ml)
D
Caspase 1 activity in Hippocampus (Units)
E
Light-Dark Test: Anxiety Test
Control Male
Control Female
Psychosocial stress Male
Psychosocial stress Female
Dark/Light Ratio
F
Open Field Test: Anxiety Test
Time spent in central area of open field (seconds)
G
Y-Maze Test: Working Memory Test
Exploratory preference (% time in novel arm)
H
Males
Fear Acquisition
Fear Extinction
Fear Recall
Control
Psychosocial stress
Control - Wedelolactone
Psychosocial stress - Wedelolactone
Freezing response (%)
Trials
I
Females
Control-Wedelolactone
Psychosocial stress -Wedelolactone

Figure 4

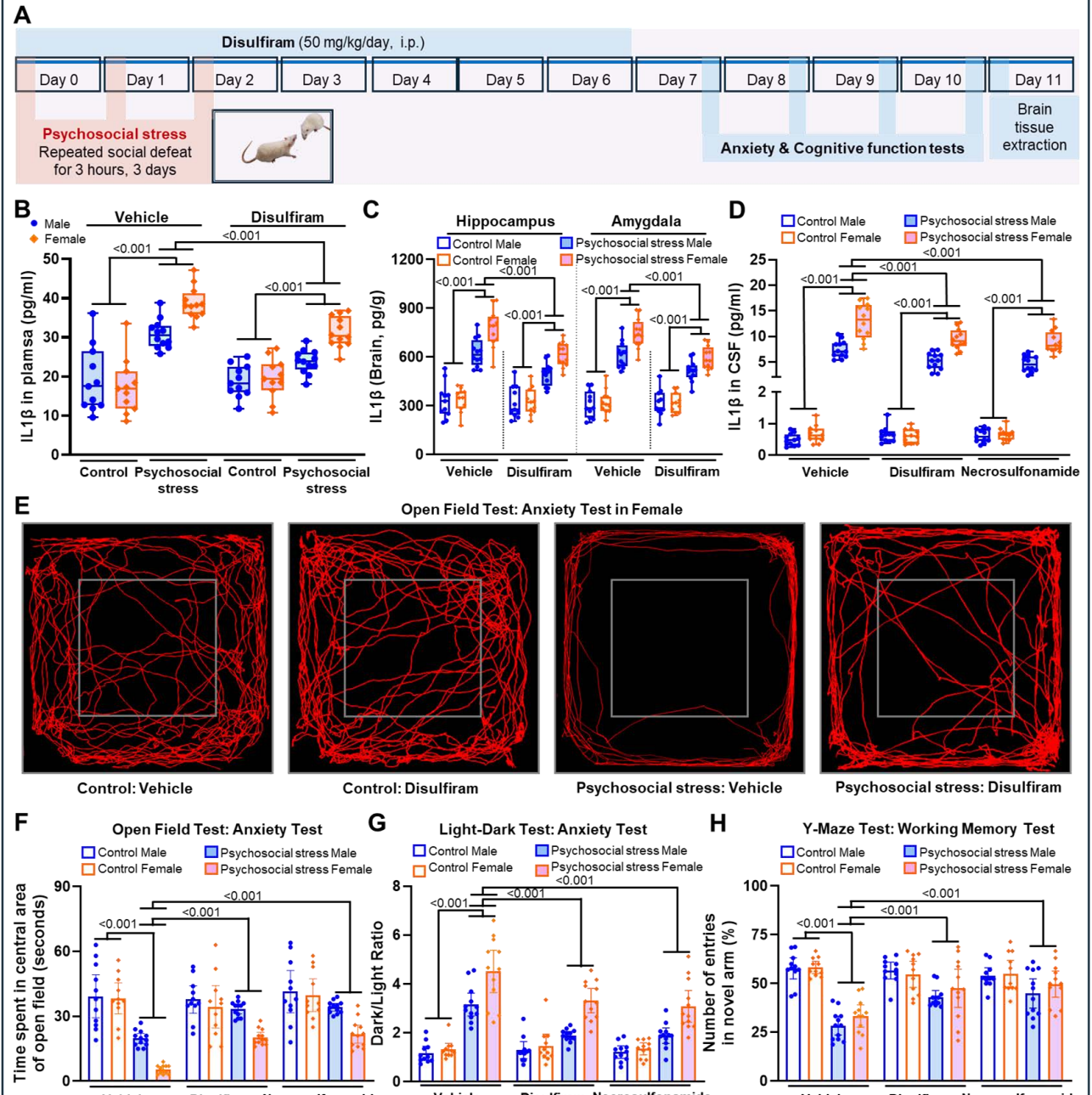
A
Disulfiram (50 mg/kg/day, i.p.)
Day 0
Day 1
Day 2
Day 3
Day 4
Day 5
Day 6
Day 7
Day 8
Day 9
Day 10
Day 11
Psychosocial stress
Repeated social defeat for 3 hours, 3 days
Anxiety & Cognitive function tests
Brain tissue extraction
B
Male
Female
Vehicle
Disulfiram
IL1β in plamsa (pg/ml)
<0.001
Control
Psychosocial stress
C
Hippocampus
Amygdala
Control Male
Control Female
Psychosocial stress Male
Psychosocial stress Female
IL1β (Brain, pg/g)
Vehicle
Disulfiram
D
IL1β in CSF (pg/ml)
Necrosulfonamide
E
Open Field Test: Anxiety Test in Female
Control: Vehicle
Control: Disulfiram
Psychosocial stress: Vehicle
Psychosocial stress: Disulfiram
F
Open Field Test: Anxiety Test
Time spent in central area of open field (seconds)
G
Light-Dark Test: Anxiety Test
Dark/Light Ratio
H
Y-Maze Test: Working Memory Test
Number of entries in novel arm (%)

Figure 5

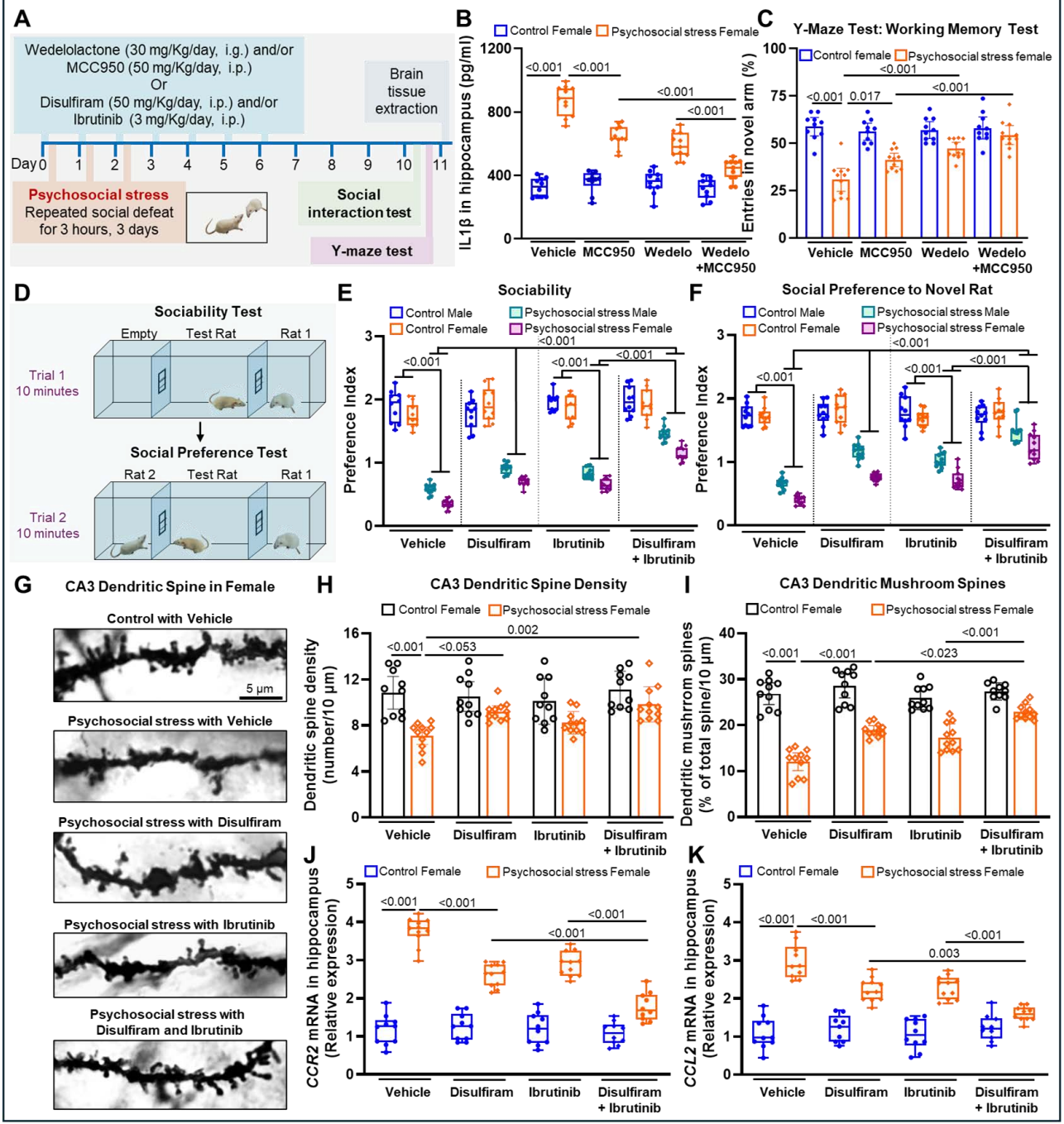
A
Wedelolactone (30 mg/Kg/day, i.g.) and/or
MCC950 (50 mg/Kg/day, i.p.)
Or
Disulfiram (50 mg/Kg/day, i.p.) and/or
Ibrutinib (3 mg/Kg/day, i.p.)
Brain tissue extraction
Day 0 1 2 3 4 5 6 7 8 9 10 11
Psychosocial stress
Repeated social defeat for 3 hours, 3 days
Social interaction test
Y-maze test
B
Control Female
Psychosocial stress Female
IL1β in hippocampus (pg/ml)
Vehicle
MCC950
Wedelo
Wedelo +MCC950
C
Y-Maze Test: Working Memory Test
Control female
Psychosocial stress female
Entries in novel arm (%)
D
Sociability Test
Empty
Test Rat
Rat 1
Trial 1
10 minutes
Social Preference Test
Rat 2
Test Rat
Rat 1
Trial 2
10 minutes
E
Sociability
Control Male
Control Female
Psychosocial stress Male
Psychosocial stress Female
Preference Index
Vehicle
Disulfiram
Ibrutinib
Disulfiram + Ibrutinib
F
Social Preference to Novel Rat
G
CA3 Dendritic Spine in Female
Control with Vehicle
5 μm
Psychosocial stress with Vehicle
Psychosocial stress with Disulfiram
Psychosocial stress with Ibrutinib
Psychosocial stress with Disulfiram and Ibrutinib
H
CA3 Dendritic Spine Density
Dendritic spine density (number/10 μm)
I
CA3 Dendritic Mushroom Spines
Dendritic mushrrom spines (% of total spine/10 μm)
J
CCR2 mRNA in hippocampus (Relative expression)
K
CCL2 mRNA in hippocampus (Relative expression)

Figure 6

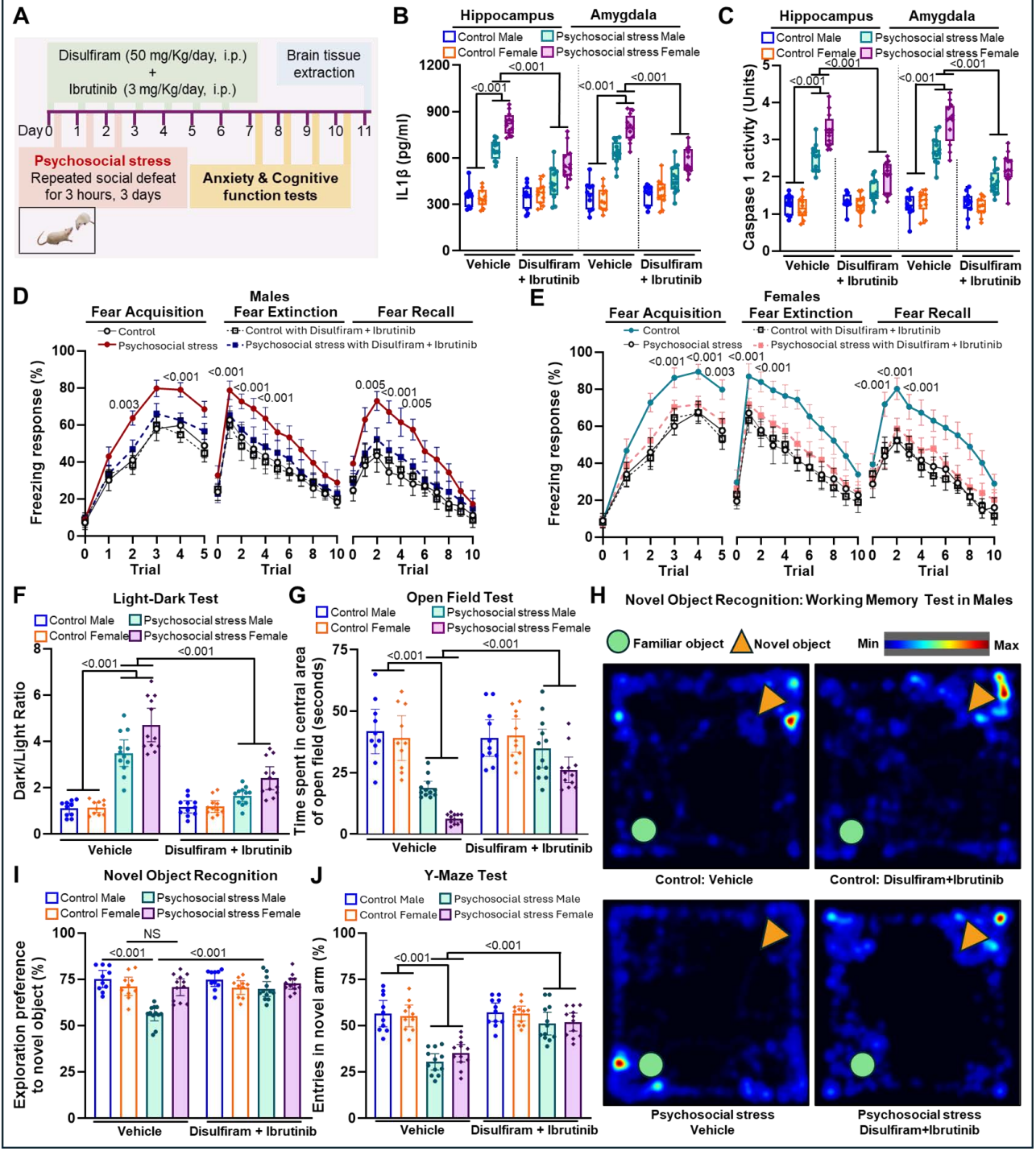
A
Disulfiram (50 mg/Kg/day, i.p.)
+
Ibrutinib (3 mg/Kg/day, i.p.)
Brain tissue extraction
Day 0 1 2 3 4 5 6 7 8 9 10 11
Psychosocial stress
Repeated social defeat for 3 hours, 3 days
Anxiety & Cognitive function tests
B
Hippocampus
Amygdala
Control Male
Control Female
Psychosocial stress Male
Psychosocial stress Female
IL1β (pg/ml)
Vehicle
Disulfiram + Ibrutinib
C
Caspase 1 activity (Units)
D
Males
Fear Acquisition
Fear Extinction
Fear Recall
Control
Psychosocial stress
Control with Disulfiram + Ibrutinib
Psychosocial stress with Disulfiram + Ibrutinib
Freezing response (%)
Trial
E
Females
F
Light-Dark Test
Dark/Light Ratio
G
Open Field Test
Time spent in central area of open field (seconds)
H
Novel Object Recognition: Working Memory Test in Males
Familiar object
Novel object
Min
Max
Control: Vehicle
Control: Disulfiram+Ibrutinib
Psychosocial stress Vehicle
Psychosocial stress Disulfiram+Ibrutinib
I
Novel Object Recognition
Exploration preference to novel object (%)
NS
J
Y-Maze Test
Entries in novel arm (%)

Figure 7

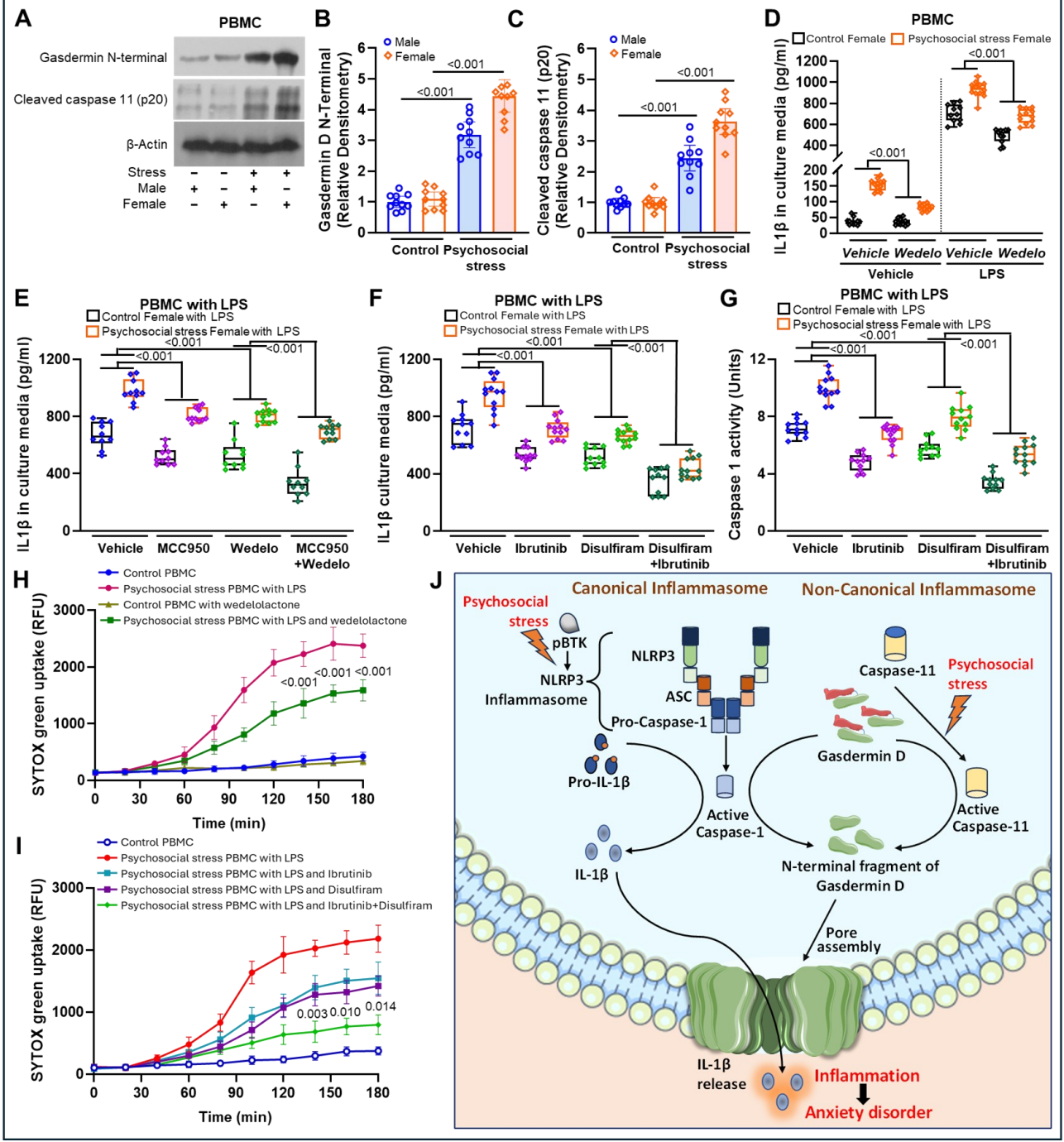
A
PBMC
Gasdermin N-terminal
Cleaved caspase 11 (p20)
β-Actin
Stress
Male
Female
B
Male
Female
Gasdermin D N-Terminal (Relative Densitometry)
<0.001
Control
Psychosocial stress
C
Cleaved caspase 11 (p20) (Relative Densitometry)
D
PBMC
Control Female
Psychosocial stress Female
IL1β in culture media (pg/ml)
Vehicle
Wedelo
LPS
E
PBMC with LPS
Control Female with LPS
Psychosocial stress Female with LPS
IL1β in culture media (pg/ml)
Vehicle
MCC950
Wedelo
MCC950 +Wedelo
F
IL1β culture media (pg/ml)
Ibrutinib
Disulfiram
Disulfiram +Ibrutinib
G
Caspase 1 activity (Units)
H
Control PBMC
Psychosocial stress PBMC with LPS
Control PBMC with wedelolactone
Psychosocial stress PBMC with LPS and wedelolactone
SYTOX green uptake (RFU)
Time (min)
I
Psychosocial stress PBMC with LPS and Ibrutinib
Psychosocial stress PBMC with LPS and Disulfiram
Psychosocial stress PBMC with LPS and Ibrutinib+Disulfiram
0.003
0.010
0.014
J
Canonical Inflammasome
Non-Canonical Inflammasome
Psychosocial stress
pBTK
NLRP3
Inflammasome
ASC
Pro-Caspase-1
Pro-IL-1β
Active Caspase-1
IL-1β
Caspase-11
Gasdermin D
Active Caspase-11
N-terminal fragment of Gasdermin D
Pore assembly
IL-1β release
Inflammation
Anxiety disorder

Supplementary Figure 1

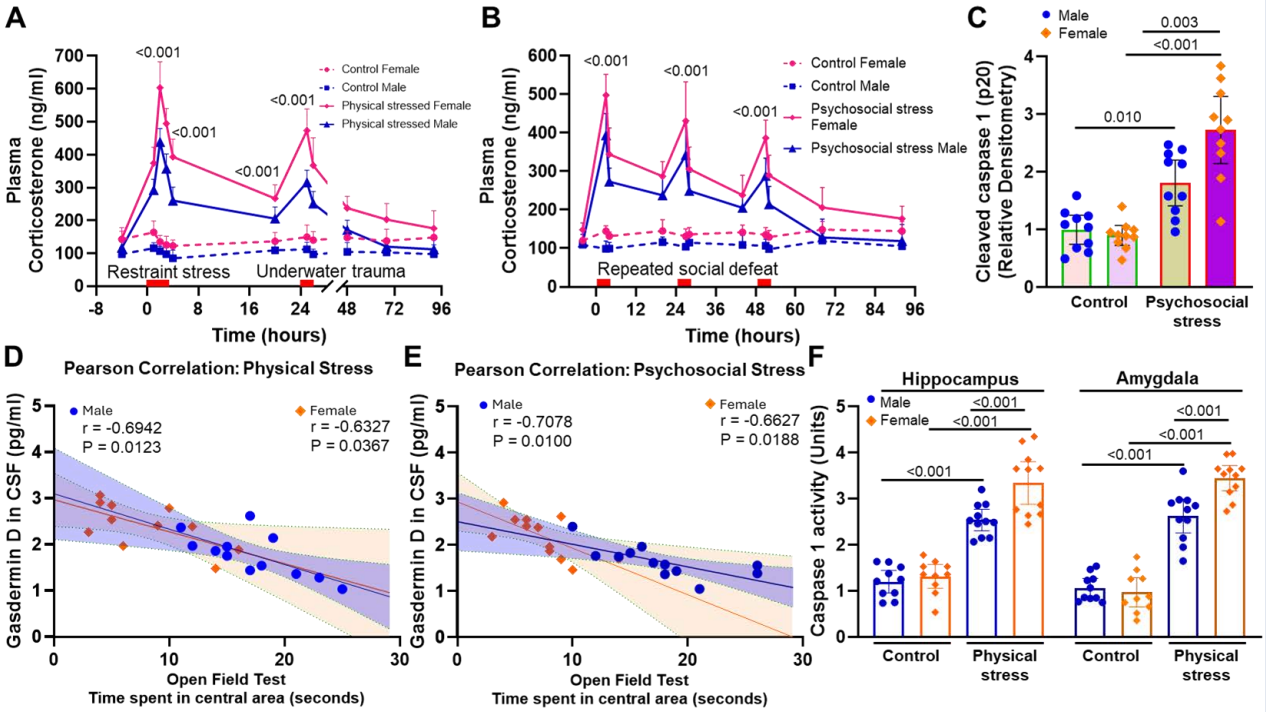

Supplementary Figure 2

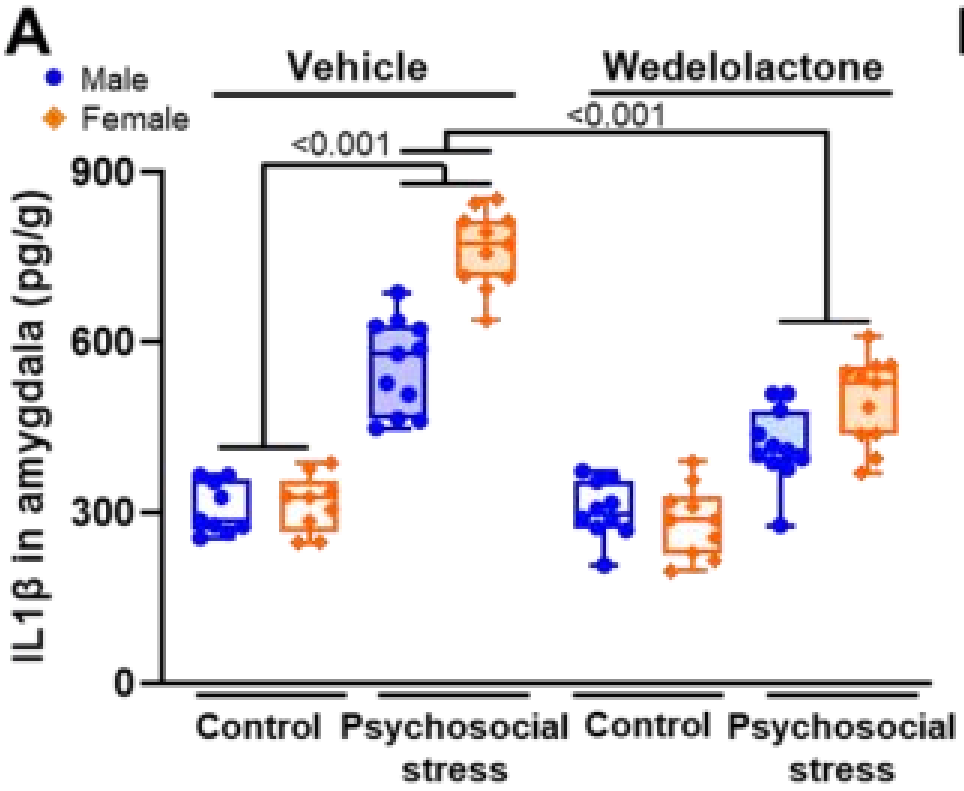

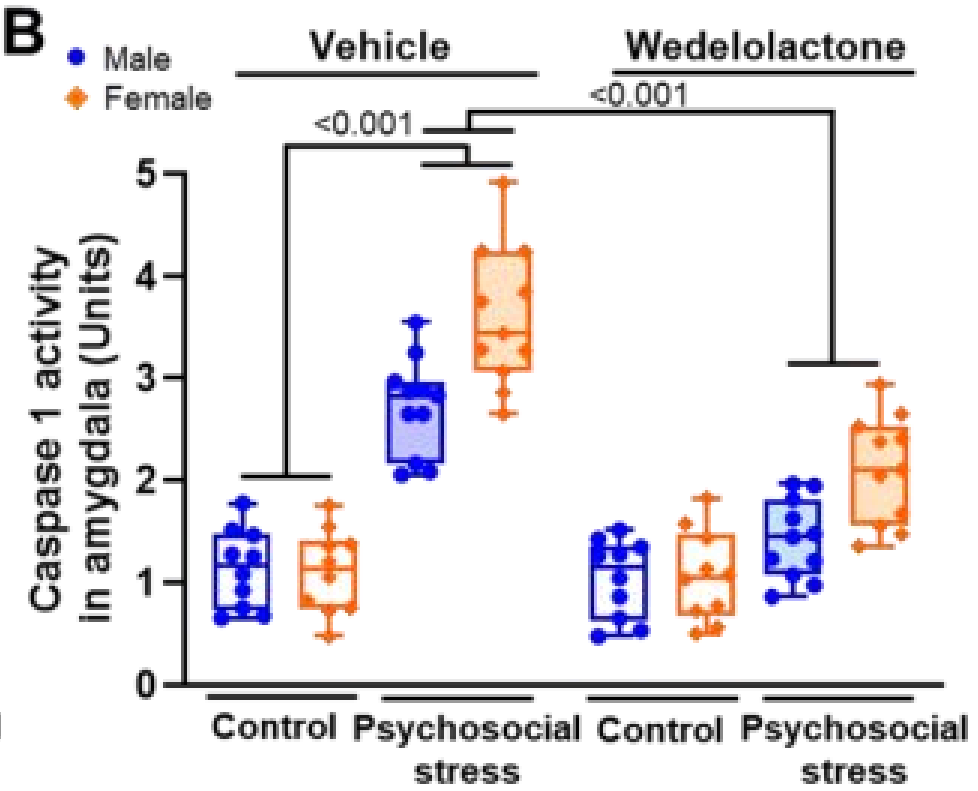

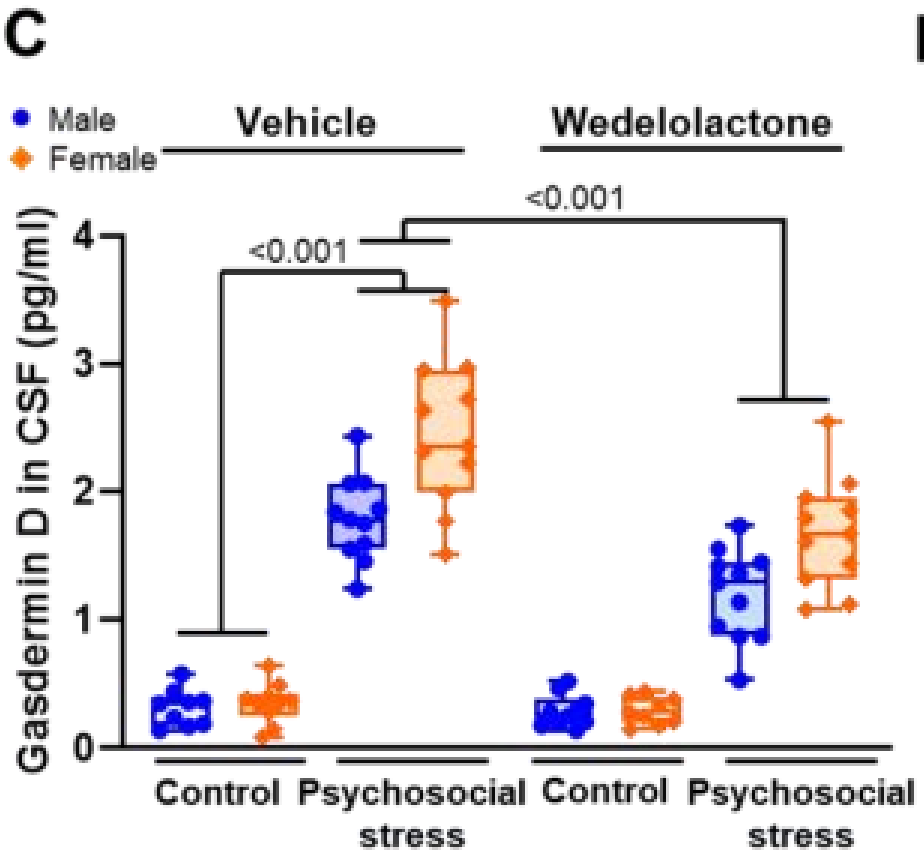

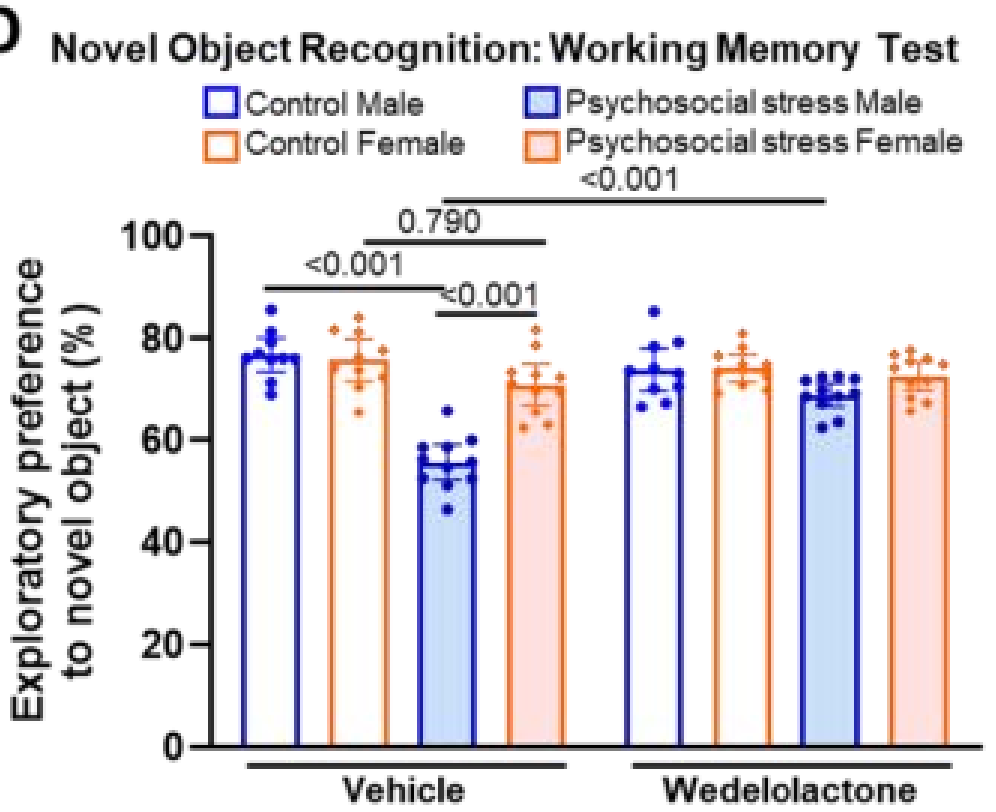

Supplementary Figure 3

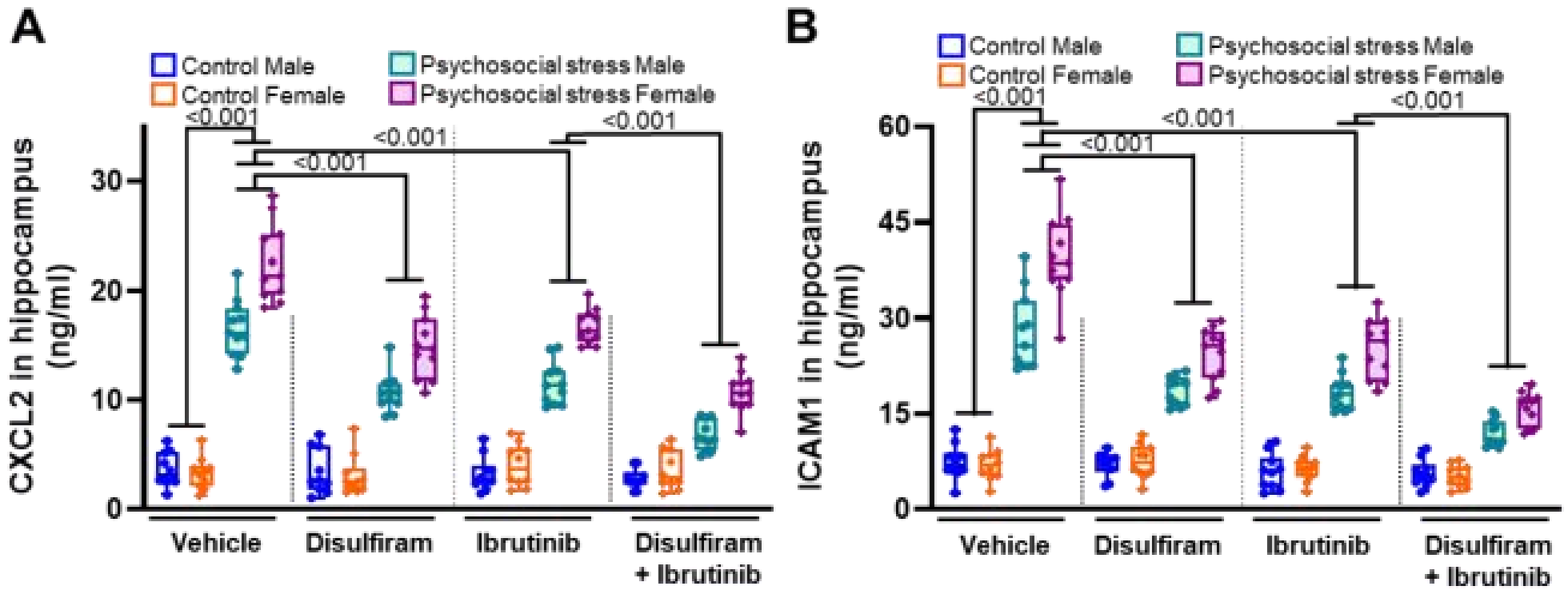

Supplementary Figure 4

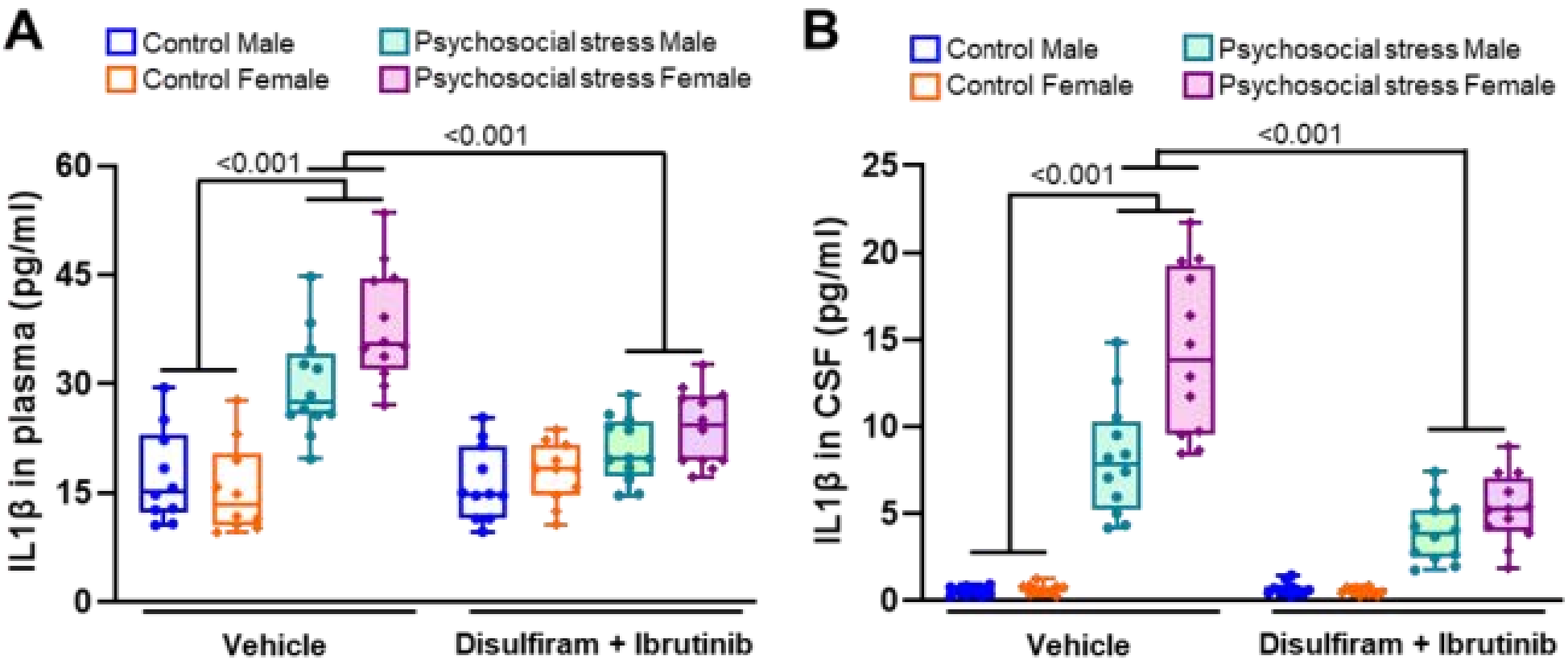
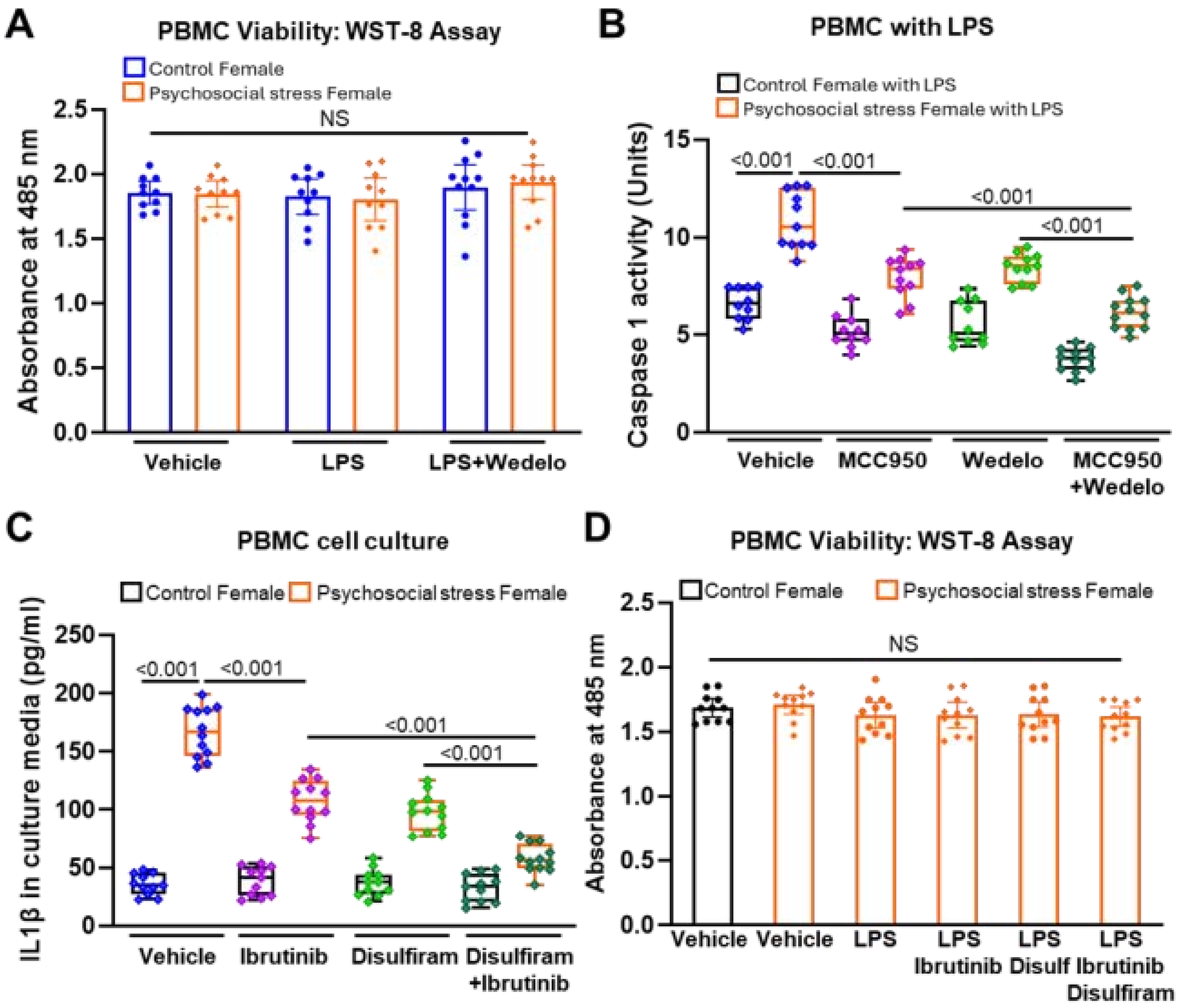
Supplementary Figure 5